Abdominal Radiology (2020) 45:457–478
https://doi.org/10.1007/s00261-019-02390-9

REVIEW

Pitfalls in the MDCT of pancreatic cancer: strategies for minimizing errors

Arya Haj-Mirzaian[1] · Satomi Kawamoto[1] · Atif Zaheer[1] · Ralph H. Hruban[2] · Elliot K. Fishman[1] · Linda C. Chu[1]

Published online: 2 January 2020

Abstract

Multidetector computed tomography (MDCT) is a widely used cross-sectional imaging modality for initial evaluation of patients with suspected pancreatic ductal adenocarcinoma (PDAC). However, diagnosis of PDAC can be challenging due to numerous pitfalls associated with image acquisition and interpretation, including technical factors, imaging features, and cognitive errors. Accurate diagnosis requires familiarity with these pitfalls, as these can be minimized using systematic strategies. Suboptimal acquisition protocols and other technical errors such as motion artifacts and incomplete anatomical coverage increase the risk of misdiagnosis. Interpretation of images can be challenging due to intrinsic tumor features (including small and isoenhancing masses, exophytic masses, subtle pancreatic duct irregularities, and diffuse tumor infiltration), presence of coexisting pathology (including chronic pancreatitis and intraductal papillary mucinous neoplasm), mimickers of PDAC (including focal fatty infiltration and focal pancreatitis), distracting findings, and satisfaction of search. Awareness of pitfalls associated with the diagnosis of PDAC along with the strategies to avoid them will help radiologists to minimize technical and interpretation errors. Cognizance and mitigation of these errors can lead to earlier PDAC diagnosis and ultimately improve patient prognosis.

Keywords Pancreatic ductal adenocarcinoma · Pancreas · Adenocarcinoma · Multidetector computed tomography · Diagnostic errors · Diagnosis

Introduction

Pancreatic ductal adenocarcinoma (PDAC) is currently the 3rd most common cause of cancer death in the USA, with the overall 5-year survival rate of 8.2% [1, 2]. With the incidence of 12.5 per 100,000 population/year, PDAC has ranked the 12th most common cancer type in the USA [3, 4]. Surgical resection is the only available curative treatment for PDAC [5–7]; however, the majority of diagnosed PDACs are not resectable at the time of diagnosis due to the advanced stage of disease which can be exacerbated by delays in diagnosis [8]. Therefore, early detection of PDAC is critical for improving the prognosis of PDAC patients. It has been shown that early diagnosis followed by surgical resection/chemotherapy significantly improves the 5-year survival rate of PDAC to as high as 30% [9].

Cross-sectional imaging has become crucial in the screening, diagnosis, staging, and prediction of resectability of PDAC [10, 11]. Multidetector computed tomography (MDCT) and magnetic resonance imaging (MRI) are the most commonly used modalities for initial assessment of patients for whom there is a clinical suspicion of PDAC [10–12]. The reported sensitivity of MDCT and MRI for the detection of PDAC ranges from 76 to 96% [13]. The diagnosis of PDAC is routinely made based on the presence of hypoenhancing pancreatic mass (as the classic primary finding) as well as several secondary imaging features including pancreatic duct dilatation, abrupt pancreatic duct caliber change, upstream pancreatic parenchymal atrophy, "double duct" sign, and vascular encasement and narrowing [14, 15].

Even with the advancements in imaging techniques, accurate diagnosis is not made in some cases which may lead to delayed diagnosis and, all too often, a missed opportunity for

✉ Linda C. Chu
lchu1@jhmi.edu

[1] Russell H. Morgan Department of Radiology and Radiological Science, Johns Hopkins University School of Medicine, Baltimore, MD, USA

[2] Sol Goldman Pancreatic Cancer Research Center, Department of Pathology, Johns Hopkins University School of Medicine, Baltimore, MD, USA

curative surgery. The accuracy of imaging in diagnosing and staging of PDAC depends on the acquisition protocol/technique and experience of the interpreter. In a study reviewing the medical records of 203 PDAC patients referred to a tertiary center, new imaging or re-evaluation of submitted images showed that 18.7% of patients had a change in their clinical stage [16]. Among these patients, 13% of them were thought to have an advanced/unresectable PDAC which was resectable in further assessments [16]. Retrospective review of cross-sectional images of PDAC patients also suggests that early signs of PDAC (such as subtle mass and inhomogeneous parenchyma) are present up to 34 months before clinical diagnosis [17]. Unfortunately, imaging features of early PDAC can be easily overlooked even by experienced radiologists and detection of early PDAC is challenging due to various technical variations as well as interpretation errors. Mitigation of these errors will have a profound impact on timely diagnosis and could improve patient survival. Radiologists should be familiar with such pitfalls in the diagnosis of PDAC to ensure optimal patient care.

In this article, we discuss and illustrate potential pitfalls in detection of PDAC using MDCT and other cross-sectional modalities. We review a variety of common technical errors including suboptimal imaging techniques, motion artifacts, incomplete anatomical coverage, as well as interpretation errors including misinterpretation related to intrinsic tumor features, coexisting and/or underlying pathologies, cognitive errors, and mimickers. We also offer strategies to avoid these pitfalls and minimize errors in the diagnosis of PDAC.

Technical errors

Recommended imaging technique and related technical challenges

MDCT with intravenous contrast enhancement is the most commonly used and best-validated modality to detect and stage PDAC [10, 18, 19]. Pooled analysis of published literature showed that the overall sensitivity and specificity of MDCT for detection of PDAC is 90% and 97%, respectively [13]. Furthermore, predicting resectability of PDAC by MDCT is estimated to be 81–91% [20–22].

Heterogeneous techniques and protocols have been used for MDCT image acquisition; Table 1 summarizes the consensus recommendation and protocol used at our institution. Table 2 also listed types of technical and interpretation errors and strategies to avoid them.

In general, biphasic MDCT examination is recommended by the Society of Abdominal Radiology and American Pancreatic Association consensus statement for initial assessment of patients with suspected PDAC [10, 11, 18]. Biphasic technique includes image acquisitions at pancreatic parenchymal or late arterial phase, and at portal venous phase. Image acquisition is performed following fast injection of high iodine concentration IV contrast (> 300 mg I/mL) through an 18–20 gauge catheter with the injection rate of 3–5 mL/s [10, 11, 18, 19]. The pancreatic parenchymal or late arterial phase images are acquired at 40–50 s after contrast injection, allowing for optimal visualization of pancreatic parenchyma and arterial anatomy and helping to detect pancreatic neuroendocrine tumors (PanNETs). The portal venous phase images are acquired at 60–90 s after contrast injection, and can be used to assess venous structures which might be critical for surgical planning and to detect metastatic liver lesions. The rationale for using biphasic technique is that the difference between the hypoattenuating tumor and enhancing normal pancreatic parenchyma is the highest during the late arterial phase which provides a clear distinction between hypodense tumor lesion and normal pancreatic parenchyma (Fig. 1) [10, 11, 18, 19]. Therefore, arterial phase images are critical for tumor visualization and accurate diagnosis.

The degree of parenchymal enhancement in biphasic technique can be affected by several technical errors such as the inappropriate volume, concentration, and rate of injection of

Table 1 Multidetector computed tomography (MDCT): biphasic pancreatic protocol parameters according to the consensus

Parameter	Consensus recommendation	Protocol at our institution
Section thickness	Submillimeter (0.5–1 mm)	0.6 mm
Oral contrast	Neutral or low-Hounsfield oral agent	1000 mL water
Intravenous contrast	High iodine concentration (> 300 mg I/mL) Injection rate 3–5 mL/s	100–120 mL nonionic contrast Injection rate 4–5 mL/s
Scan acquisition	Pancreatic parenchymal phase 40–50 s Portal venous phase 65–70 s	Bolus trigger off abdominal aorta at threshold of 230 Hounsfield Portal venous phase 60 s
Image reconstruction	Axial 2–5 mm MPR, MIP, 3D VR	Axial 0.75–3 mm MPR, MIP, 3D VR

Recommendation and our institution protocol

MIP maximum intensity projection, *MPR* multiplanar reformatting, *VR* volume-rendered

Table 2 Diagnostic pitfalls in the multidetector computed tomography (MDCT) of pancreatic ductal adenocarcinoma (PDAC)

	Description	Strategies for minimizing
Technical errors		
Suboptimal imaging technique		
Non-contrast MDCT	Low diagnostic accuracy for PDAC, may occur in incidentally detected pancreatic pathologies	Low threshold to refer to dedicated biphasic pancreatic MDCT protocol
Suboptimal imaging quality		
Contrast-enhanced MDCT	Inappropriate volume, concentration, and rate of injection of intravenous contrast material	Follow consensus recommendation for biphasic pancreatic MDCT protocol
High-density oral contrast	Obscure pancreatic pathologies and interfere with 3D post-processing	Use neutral or low HU oral contrast
Motion artifact	Especially in MRI (when contrast-enhanced MDCT is contraindicated), caused by respiratory, bowel, voluntary movements	Use FSE, TSE, and SSFSE sequences Use abbreviated MRI protocols Use motion artifact reduction methods Use exhalation breath-hold, delay acquisition until 10 s of breath-holding
Incomplete anatomical coverage	Especially in MRI (when contrast-enhanced MDCT is contraindicated), pancreatic head and uncinate process may be incompletely included due to variability in patients' breath-hold	Same as above
Interpretation errors		
Intrinsic tumor features		
Small tumor size	Suboptimal diagnostic performance of MDCT for detecting small (less than 20 mm) masses	Assessment of secondary signs: ductal dilation, ductal caliber change, abrupt duct cut-off, abnormal pancreas contour, pancreatic atrophy, and pancreatitis Use submillimeter thin MDCT slices Review MPR images
Exophytic mass	Exophytic pancreatic masses can be mistaken for peri-pancreatic pathologies, and vice versa	Hypoenhancement of the pancreas in contiguity with the infiltration of soft tissue is the clue to the origin of mass Use 3D images
Isoenhancing mass	Isoenhancing PDAC (difference of < 15 HU in comparison with background) is not easy to detect using MDCT	Assessment of secondary signs: abrupt caliper change, pancreatic atrophy, and pancreatitis Use 3D images Use split-bolus technique or delayed phase technique Use MRI or PET/CT
Subtle duct irregularity	Pancreatic duct irregularity, as a possible only sign of a PDAC, can be easily missed on MDCT	Use coronal and sagittal MPR images Use EUS or MRCP in the case of suspicion
Diffuse tumor infiltration	Diffuse tumor infiltration may mimic AIP, pancreatic lymphoma, and metastasis	Diffuse AIP: lack of main pancreatic duct dilation on MDCT, other AIP features such as "sausage-like" gland, presence of hypodense ''halo,' rim like enhancement, serum IgG4, response to steroids Diffuse pancreatic lymphoma: no (or mild) ductal dilatation Diffuse metastases: peripheral or homogeneous (less common) enhancement
Coexisting or underlying pathologies		

Table 2 (continued)

	Description	Strategies for minimizing
Chronic pancreatitis	Chronic pancreatitis can cause PDAC and show similar imaging features, focal mass-mimicking chronic pancreatitis the appearance of PDAC	Abrupt termination of ducts and smooth ductal dilatation are more suggestive of a PDAC on MDCT Use EUS and EUS-guided fine needle biopsy with several sampling using a large needle Conflicting data on the utility of DWI 18FDG-PET may be helpful, though it is not the first-line modality
IPMN	IPMNs can progress to PDAC; it is challenging to diagnose PDAC or predict IPMNs malignancy	Predict IPMN malignancy: nonenhancing mural nodules, solid focal components, size of ≥ 3 cm, ductal dilatation (≥ 10 mm), thick/enhanced wall and/or septum MRCP may improve detection of internal septation and mural nodules Use EUS and/or biopsy in high-risk subjects
Cognitive errors		
Distracting findings	Satisfaction of search due to pancreatitis, pancreatic cysts, IPMNs, or other findings	Aware of the possibility of satisfaction of search errors especially in the case of IPMNs and other cystic lesions
Incidental findings	Incidental findings on images performed for other clinical indications: suboptimal protocol and "edge-of-film" effect	Use the biphasic pancreatic MDCT protocol and assess the whole organ For cysts, perform EUS and/or biopsy in high-risk subjects
Mimickers of PDAC		
Focal fatty infiltration	Hypoattenuating region can simulate PDAC	Focal fat should not have associated secondary signs (e.g., pancreatic duct or common bile duct dilatation). MRI can characterize the fat signal
IPAS	It may mimic PDAC, PNET, and hypervascular metastases	IPAS mirror splenic attenuation and signal IPAS usually located at the tip or along the dorsal surface of the pancreatic tail Use arciform splenic enhancement pattern, super-paramagnetic iron oxide-enhanced MRI, Tc-99m heat-damaged red blood cell scintigraphy, and Tc-99m sulfur colloid scintigraphy
Pancreatitis	Acute and chronic pancreatitis, as well as AIP can mimic PDAC	Same as above

3D 3-dimensional, *AIP* autoimmune pancreatitis, *DWI* diffusion-weighted imaging, *FSE* fast spin echo, *HU* Hounsfield unit, *IPAS* intrapancreatic accessory spleen, *IPMNs* intraductal papillary mucinous neoplasm, *MDCT* multidetector computed tomography, *MPR* multiplanar reformatting, *MRCP* magnetic resonance cholangiopancreatography, *MRI* magnetic resonance imaging, *PDAC* pancreatic ductal adenocarcinoma, *PET* positron emission tomography, *PNET* pancreatic neuroendocrine tumors, *SSFSE* single-shot FSE, *TSE* turbo spin echo

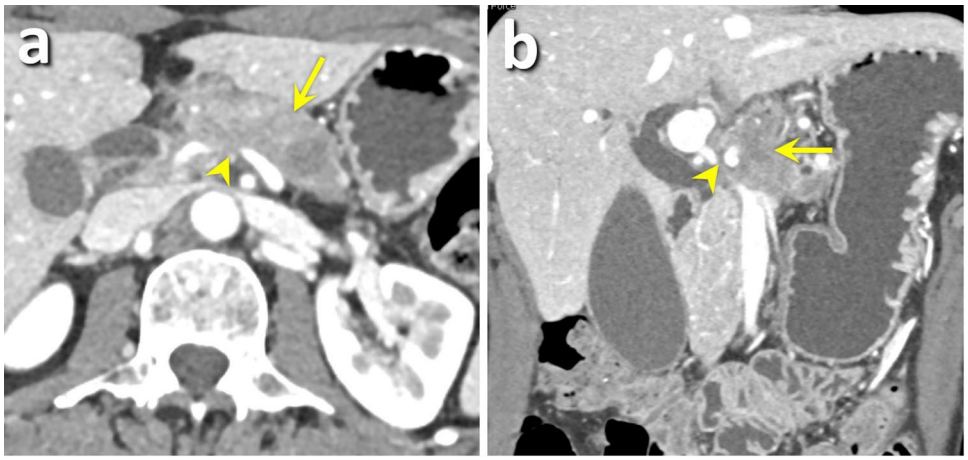

Fig. 1 A 62-year-old female with pancreatic ductal adenocarcinoma (PDAC). Arterial phase of axial (**a**) and coronal (**b**) contrast-enhanced MDCT images show diffusely infiltrative mass (yellow arrows) with encasement of celiac artery, splenic artery, common hepatic artery, as well as encasement and severe narrowing of portal superior mesenteric vein confluence (yellow arrowheads)

intravenous iodinated contrast. All such technical errors can lead to suboptimal image quality and can negatively impact diagnostic performance. Although it has been highly recommended to use both late arterial and portal venous phases for evaluation of patients with the suspected pancreatic lesion, a recent pooled analysis showed no significant difference between using both late arterial and portal venous phases versus utilizing only portal venous phase [20]. By analyzing results of 29 articles evaluating the role of MDCT in predicting resectability of PDAC, authors showed no significant difference between studies utilizing only portal venous phase versus studies using both pancreatic and portal venous phases (positive predictive value of 75% versus 84% for predicting resectability of PDAC, respectively; p-value of 0.153) [20].

Neutral or low-Hounsfield-units (HU) oral contrast is recommended to visualize the stomach and small bowel and to minimize the MDCT artifacts during image post-processing. Positive or high-density oral contrast should be avoided since it may obscure pancreatic pathologies and interfere with 3-dimensional (3D) post-processing [10, 11, 18]. Pancreatic pathology may be incidentally detected on non-contrast MDCT obtained for other clinical indications—all these lesions should be evaluated using biphasic protocol (incidentalomas are discussed in the next sections) (Fig. 2) [10, 11, 18].

Image data are obtained at a section thickness of 0.62–0.75 mm (submillimeter) and reconstructed into 2–5 mm axial slices for standard interpretation. For diagnosis and staging of PDAC, images are also routinely reconstructed to create post-processing multiplanar reconstruction (MPR) and 3D images, including maximum intensity projection (MIP) and volume-rendered (VR), which are essential for the detection of subtle changes and staging of PDAC (Fig. 3). It has been suggested that coronal and sagittal MPR images provide more accurate information about the resectability of PDAC, including vascular invasion and the relationship of the tumor to the

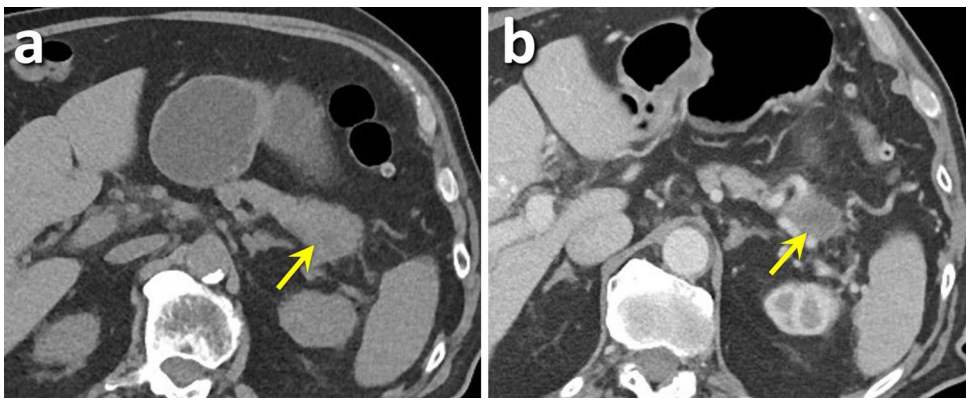

Fig. 2 A 73-year-old male presented with abdominal pain and clinical suspicion of kidney stone. Pancreatic ductal adenocarcinoma was incidentally detected on non-contrast MDCT examination with the renal stone protocol. Axial non-contrast MDCT image (**a**) shows subtle fullness of the pancreatic tail (yellow arrow). The patient was assessed with biphasic contrast-enhanced MDCT, and hypoenhancing pancreatic mass (yellow arrow) was clearly defined on the venous phase of axial contrast-enhanced MDCT image (**b**)

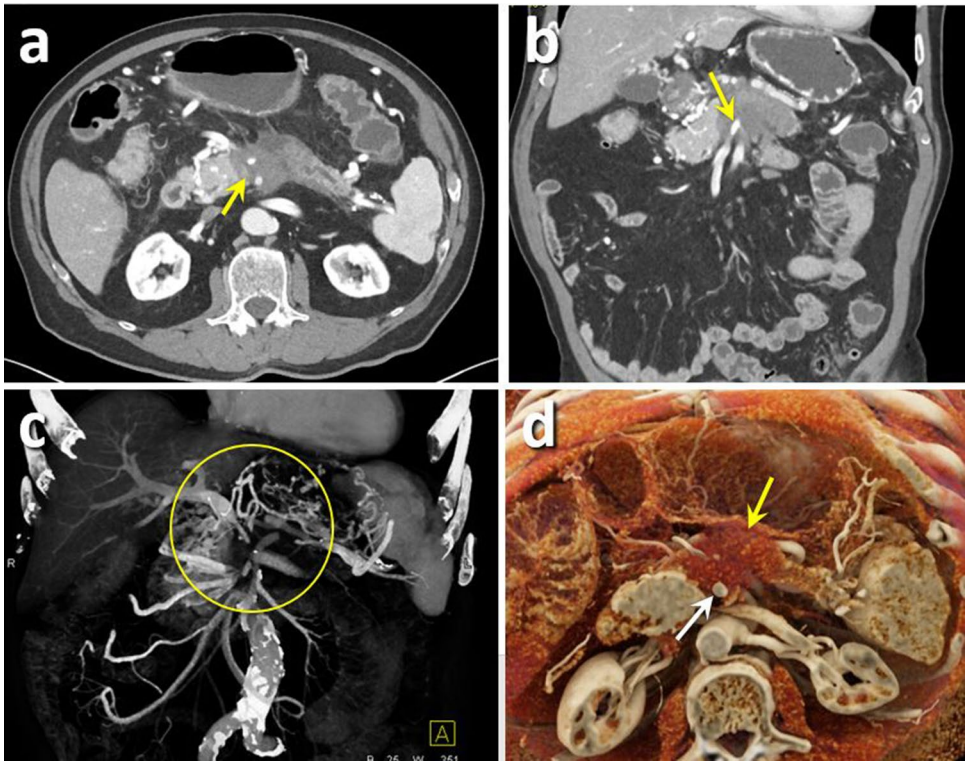

Fig. 3 An 80-year-old male with pancreatic ductal adenocarcinoma (PDAC). Arterial phase of axial (**a**) and coronal (**b**) contrast-enhanced MDCT images demonstrate encased celiac artery and superior mesenteric artery (yellow arrows), and occlusion of portal confluence with prominent venous collaterals in pancreatic head. Reconstructed 3D images were obtained for better assessment of vascular anatomy. Venous phase of coronal contrast-enhanced MDCT image with 3D reconstruction (**c**) shows vascular invasion of PDAC (yellow circle). 3D image obtained using cinematic rendering (**d**) shows tumor (yellow arrow) encasement of the celiac artery (white arrow) and prominent venous collaterals in pancreas head

superior mesenteric artery (SMA), superior mesenteric vein (SMV), and celiac axis [14, 19, 23–27]. Whereas, MIP images are optimized to assess vascular anatomy and VR images are optimal for the evaluation of soft tissues and vascular anatomy as well as complex relationships between different structures and pathologies [14, 19, 23–27]. Besides providing more accurate information regarding tumor anatomy and vascular invasion, 3D reconstructions are useful for pre-operative planning. Fang et al. showed that 3D image reconstruction had significantly higher diagnostic performance for predicting PDAC resectability when compared with CT-angiography [26]. Despite the fact that MDCT and reconstructed 3D images can be used for assessing vascular invasion, it should be noted that they are not perfect. Some studies demonstrated the lower accuracy of MDCT in evaluation of vascular invasion with the sensitivity of 60% and specificity of 94% [28]. In addition to traditional methods, cinematic rendering (CR) as a novel 3D rendering technique can be used to generate photorealistic with more accurate information regarding the anatomical details (Fig. 3) [29, 30]. CR can assist clinicians to visualize precisely the extent of tumor vascular invasion, which might be critical for surgical planning; however, the feasibility of this method and other novel techniques in routine clinical practice is yet to be studied [29, 31, 32].

Motion artifacts and incomplete anatomic coverage

MRI is usually reserved as a second-line modality for the diagnosis and staging of PDAC when contrast-enhanced MDCT is contraindicated (due to contrast allergy and/ or renal insufficiency) [11, 14]. Several studies have compared the diagnostic performance of MRI with contrast-enhanced MDCT [13, 33–36]. Most, but not all, studies have found that MDCT is more accurate in determining tumor resectability (73–87%) than MRI (70–79%) [13, 33–36]. MRI may be more sensitive for detection of liver metastasis and may be superior in detecting small PDACs [37, 38]. Despite these promising findings regarding the diagnostic performance of MRI, these images should be interpreted with caution because of the possibility of motion and other artifacts [39]. MRI is more susceptible to motion artifacts in comparison to MDCT; these motion artifacts can obscure small tumors and lead to misdiagnosis. Motion can result in image blurriness and artifacts (Fig. 4) [40, 41]. Motion can be introduced by respiratory movements, bowel movements, voluntary movements, and cardiac and vascular pulsations [39, 42]. Motion artifact can be categorized into ghost artifact, and artifacts due to randomly moving structures (e.g., bowel movement), repetitive motion (e.g., respiration), and moving fluid within defined spaces (e.g., vessels) [43, 44]. Each of these artifacts has its specific imaging features and radiologists must be

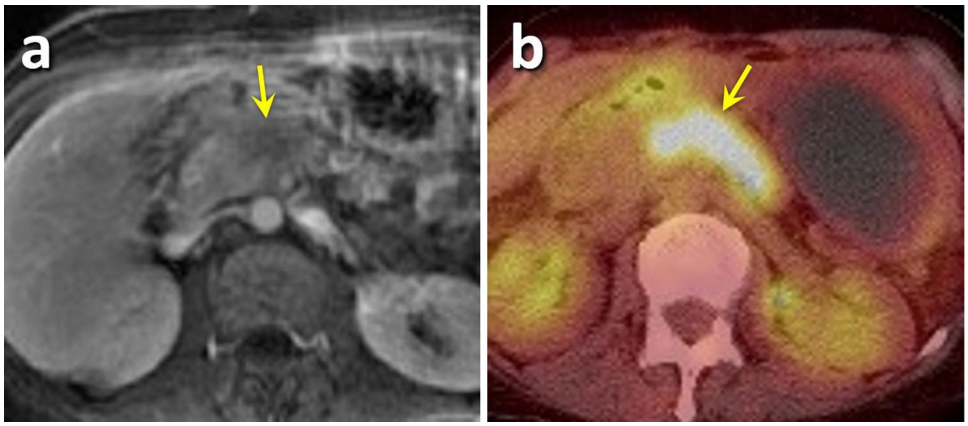

Fig. 4 A 67-year-old female with suspected pancreatic ductal adenocarcinoma (PDAC). The patient underwent MRI and PET/CT examinations, because of contrast allergy. Respiratory motion artifact and blurry margins of the pancreatic mass (yellow arrows) were seen on axial post-gadolinium T1-weighted MR (**a**) and axial fused PET/CT (**b**) images, which made it difficult to evaluate local vascular involvement (a critical element of cancer staging) of PDAC

familiar with the basic principles of abdominal MRI artifacts [43].

Several methods have been introduced to minimize motion artifacts, including direct correction (i.e., physical restraint, sedation, and antiperistaltic agents), respiratory and cardiac gating, minimizing acquisition time, suppression of signal in moving structures, signal averaging, and swapping the phase and frequency-encoding axes [43, 44]. However, no method can completely suppress MRI motion artifacts and radiologists should be aware of imaging features of artifacts in order to prevent interpretation errors [43]. Furthermore, the pancreatic head and uncinate process may be incompletely included in axial MRI due to variability in patients' breath-hold (Fig. 5). In this regard, it has been

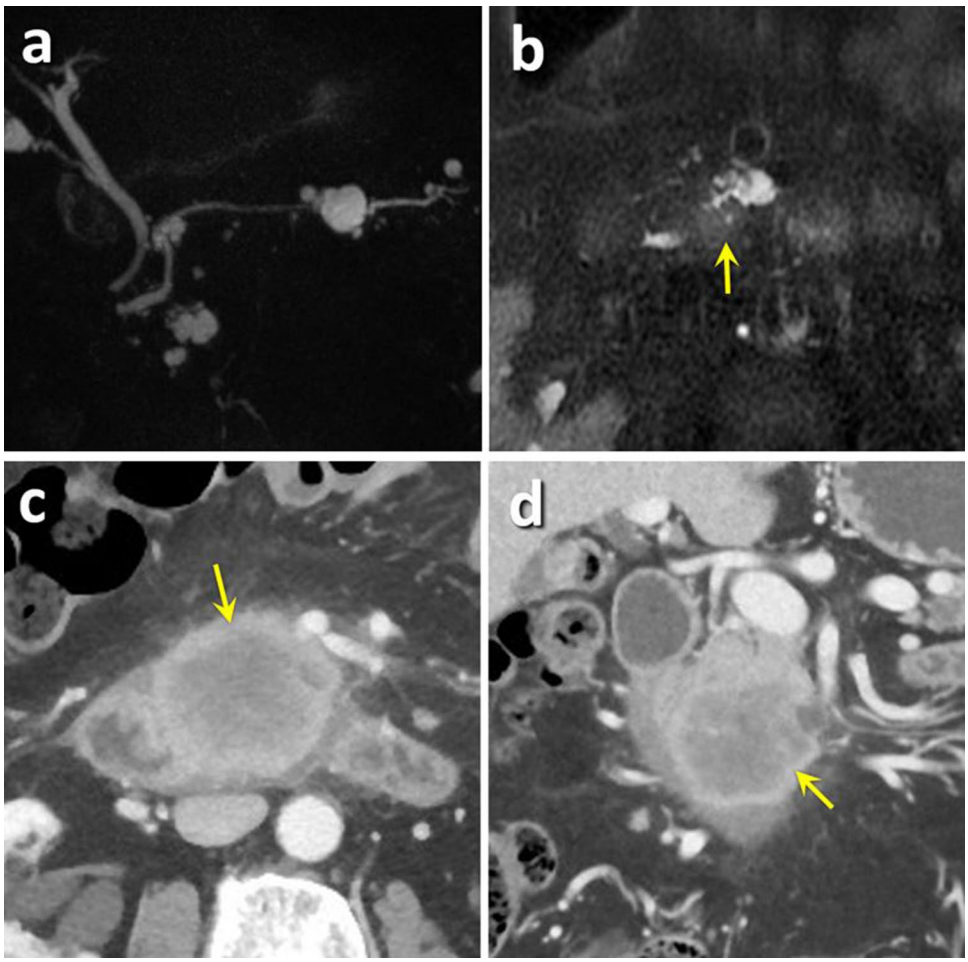

Fig. 5 An 86-year-old male with intraductal papillary mucinous neoplasm (IPMN) who was followed up with MRI and MDCT examinations. Coronal MIP MRCP image (**a**) shows subtle hyperintense mass, which was partially visualized on axial T2-weighted MR image (**b**) (yellow arrow). Follow-up MDCT examination 10-months later reveals locally advanced pancreatic ductal adenocarcinoma on the venous phase of axial (**c**) and coronal (**d**) contrast-enhanced MDCT images (yellow arrows)

shown that fast and turbo SE (FSE and TSE) sequences (with the lower acquisition time) are less prone to these artifacts [43–45]. Furthermore, image acquisition of single-shot FSE (SSFSE) is performed using a single breath-hold which results in decreased motion artifacts and better anatomic coverage when compared with FSE (typically takes 5–7 min) [45]. Lens et al. demonstrated that exhalation breath-hold (in comparison with inhalation breath-hold) and delaying acquisition until first 10 s of breath-holding might reduce the magnitude of pancreas and diaphragm motion and result in more stable anatomy [39]. Also, large body of evidence suggested using abbreviated MRI protocols (rather than the standard protocol) may improve MRI quality by reducing motion artifacts [46]. Due to the possibility of incomplete anatomy coverage, MRI technologists must be educated to recognize incomplete coverage through quality assurance.

The usefulness of positron emission tomography (PET)/CT with F-18-fluorodeoxyglucose (FDG) for diagnosis of PDAC has been evaluated in a limited number of studies, and PET/CT may have an equivalent diagnostic accuracy compared to other cross-sectional imaging modalities [47, 48]. However, it should be noted that using PET/CT also subjects to respiratory motion artifacts which is a major issue regarding the diagnostic performance and accuracy in staging [49].

Interpretation errors

Interpretation challenges due to intrinsic tumor features

Small tumor size

The survival of patients with small PDACs (particularly ≤ 20 mm), 30% at 5 years, is better than it is for patients with larger cancers [50, 51]. However, small tumors are the most difficult to visualize and the sensitivity of MDCT is lower for detection of small PDACs (Fig. 6) [52, 53]. In a retrospective study by Yoon et al. with 33 PDAC patients who underwent CT prior to the diagnosis of PDAC, the tumor could be identified in 72.7% (24/33) of cases. Of these prospectively missed cases, 87.5% (21/24) were ≤ 20 mm and 12.5% (3/24) were between 21 and 33 mm. [54]. In such cases, we can use two approaches; first, reviewing submillimeter thin MDCT slices and MPR images to minimize volume averaging and improve visualization of small masses [14, 23–26]. Second, secondary signs are critical in detecting small PDACs [12, 17, 55, 56].

Using thin collimation technique and submillimeter slice section allows small tumors to be visualized better

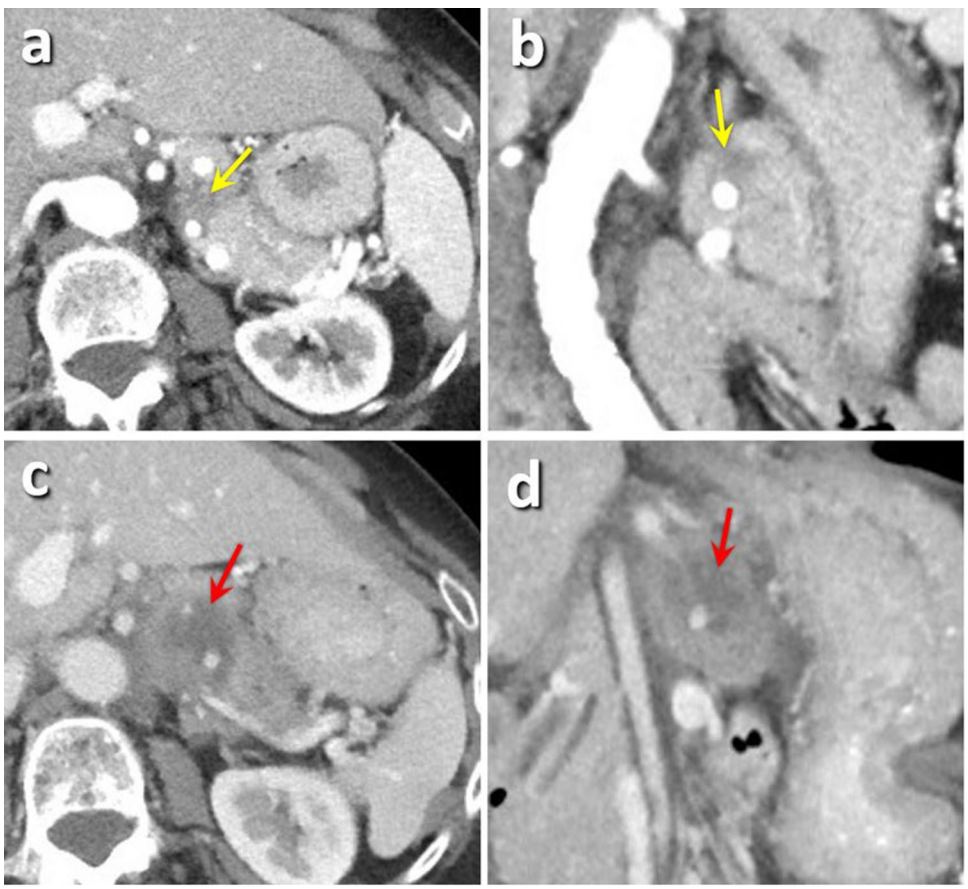

Fig. 6 A 74-year-old female admitted with abdominal pain and clinical suspicion of pancreatic ductal adenocarcinoma (PDAC). The patient underwent contrast-enhanced MDCT examination which was interpreted as normal, and a subtle hypoattenuating pancreatic lesion (yellow arrows) was missed on venous phase of axial (**a**) and coronal (**b**) contrast-enhanced MDCT images. Follow-up MDCT examination 8 months later shows locally advanced PDAC (red arrows) on venous phase of axial (**c**) and coronal (**d**) contrast-enhanced MDCT images

[14, 23, 24]. However, utilizing thin-slice sections has some inherent limitations. It has been shown that thin-section datasets were significantly larger regarding the volume of the images and it took longer to retrieve, reconstruct, and interpret these images [57, 58]. Moreover, it has been demonstrated that thin-section CT images were less tolerant of compression and had more artifacts in comparison with thick-section images [59]. In this regard, several strategies such as limiting thin slices to one imaging plane and using iterative reconstruction techniques can be utilized to compensate these limitations. Several studies also suggested that 3D and MPR reconstructions improve the conspicuity of small PDACs [14, 23, 24]. 3D images also have advantages in visualizing small tumors located at the junction of pancreatic and common bile ducts, which can be difficult to detect using axial or MPR images [14, 23–26]. Regarding the secondary signs, the presence of common bile duct and main pancreatic ductal dilatation, pancreatic ductal caliber change and abrupt duct cut-off at the level of the tumor, abnormal pancreas contour, pancreatic atrophy, and pancreatitis are highly suspicious for small PDACs, even in the absence of a clearly defined mass (Fig. 7) [17, 55, 56]. Yoon et al. showed that secondary signs could be a solution to the concerns associated with detecting small PDACs [54]. They demonstrated that 76% of small PDAC had secondary signs—with main pancreatic duct or common bile duct dilatation (63%), abrupt pancreatic duct cut-off (63%), parenchymal atrophy (21%), and contour abnormality (14%) [54].

Exophytic mass

A large spectrum of benign or malignant lesions of the pancreas can have an exophytic appearance on imaging. Up to 58% of PDAC are partially exophytic [60]. Furthermore, pancreatic acinar cell carcinoma (ACC) are mainly characterized by their exophytic features [61, 62]. These exophytic pancreatic masses with infiltrative growth pattern can be mistaken for peri-pancreatic lymph nodes, metastatic lymphadenopathy, lymphoma, neurogenic tumors, duodenal cancers, gastrointestinal stromal tumor (GIST), or diverticula, gastric masses, and primary retroperitoneal masses and vice versa—all these entities could also be confused with exophytic PDAC on axial images. Subtle hypoenhancement of the pancreas in contiguity with the infiltration of soft tissue is the clue to the origin of exophytic mass (Fig. 8) [15, 23].

Isoenhancing mass

PDACs can sometimes be isoenhancing, and when they are, they are often misdiagnosed or unrecognized (Figs. 7 and 9). Isoenhancing mass is defined as a lesion with an attenuation difference of < 15 HU in comparison with background parenchyma in all phases [63, 64]. It has been shown that 5–45% of PDACs are isoattenuating relative to the remainder pancreatic parenchyma on both late arterial and portal venous phases [63, 65, 66]. Isoenhancement is more commonly seen in smaller tumors, which make the diagnosis even more challenging [63, 66–68]. It should be noted that small isoattenuating PDAC should not be regarded as early cancers, since only a small proportion of these lesions are stage T1 tumors [54].

The detection of small isoattenuating PDAC relies on secondary signs including pancreatic duct abnormalities (i.e., abrupt pancreatic duct cut-off, main pancreatic duct or common bile duct dilation) and changes in the contour of the pancreas (Fig. 7) [63, 66]. Based on our experience, presence of abrupt caliber change of pancreatic duct with atrophy should be considered as equivalent to the presence of pancreatic mass until proven otherwise and warrants additional assessments. However, Tamada et al. showed that 14% of PDACs have no secondary signs [56]. They also demonstrated that isoattenuating tumors located in the uncinate process are less likely to show secondary signs of

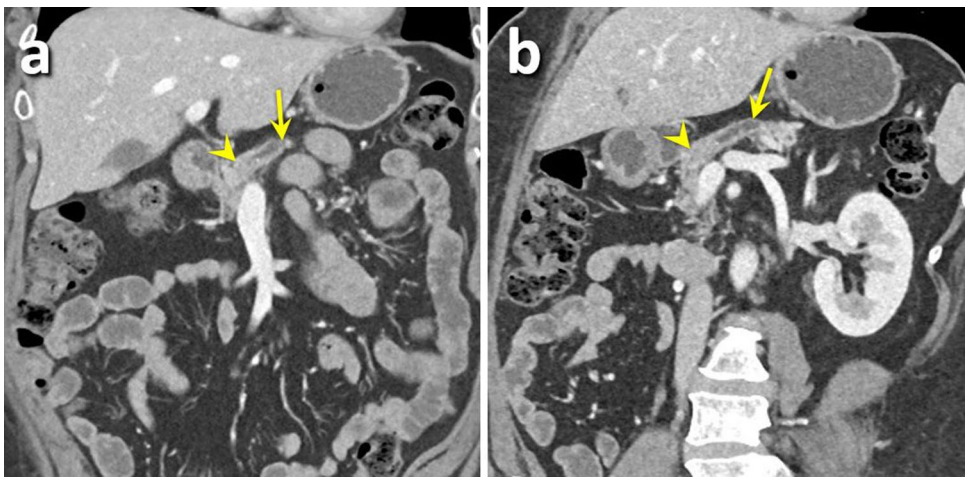

Fig. 7 Coronal (**a**) and coronal oblique (**b**) post-contrast MDCT image from a 58-year-old female with a history of renal cell carcinoma who underwent nephrectomy and were followed up with MDCT. Abrupt cut-off of the dilated pancreatic duct (yellow arrows) with a subtle hypoattenuating mass in the pancreatic neck (yellow arrowheads) (representing PDAC) was observed on follow-up images

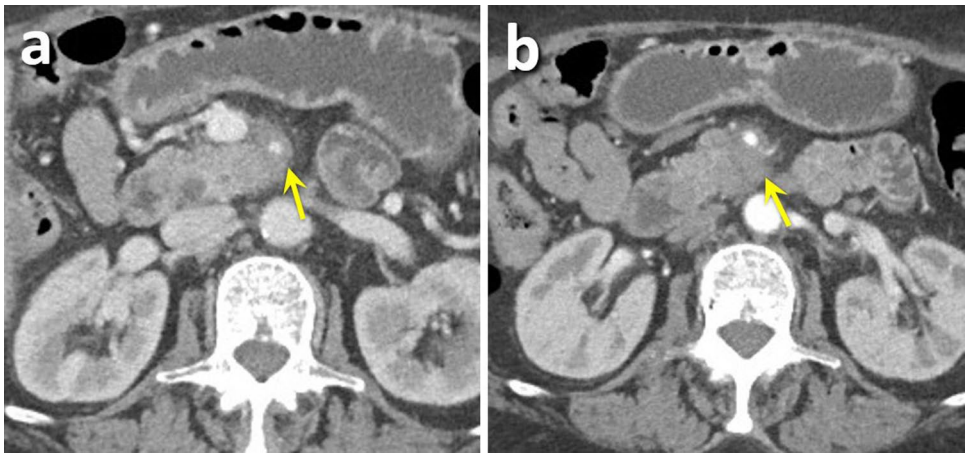

Fig. 8 Venous (**a**) and arterial (**b**) phase of axial contrast-enhanced MDCT image from a 76-year-old female with pancreatic ductal adenocarcinoma. Images show an exophytic uncinate process mass (yellow arrows)

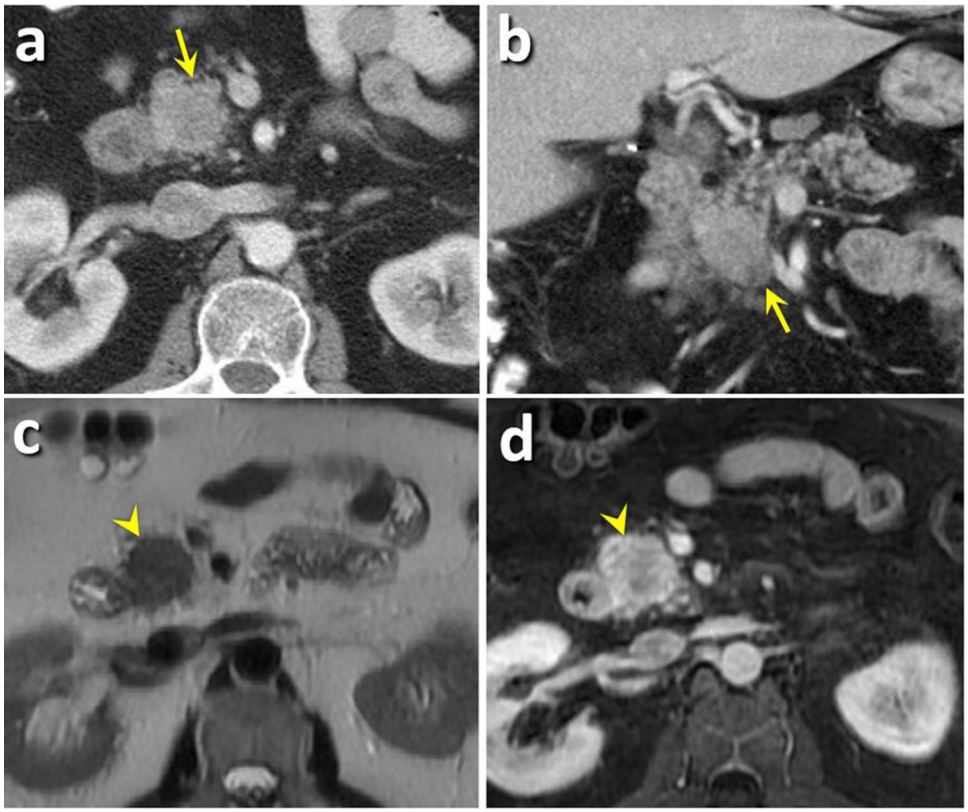

Fig. 9 Axial (**a**) and coronal (**b**), venous phase, post-contrast MDCT images from a 60-year-old male show subtle isoenhancing uncinate process mass (yellow arrows) and loss of normal fatty lobulation which was not recognized on outside CT examination. After 2-months, follow-up axial T2-weighted MR (**c**) and axial post-Gad T1-weighted MR (**d**) images from the same patient show subtle heterogeneously enhancing mass (yellow arrowheads), which was pathologically proven to be pancreatic ductal adenocarcinoma

main pancreatic duct or common bile duct obstruction [56]. Tumors located in the tail of the pancreas are less likely to demonstrate pancreatic duct dilatation. In these instances, subtle textural changes and loss of normal fatty lobulations (Figs. 9–10) may serve as clues for an underlying mass. Some reports also suggested using the split-bolus technique (combines pancreatic phase and portal venous phases in a single scan) and delayed phase technique (in which additional delayed phase in the upper abdomen is performed at 5 min) to increase the sensitivity of MDCT in the detection of small isoattenuating PDACs [68]. Furthermore, MRI and PET/CT may be helpful in this regard, with the sensitivity of 79.2% and 73.7%, respectively, for detecting isoattenuating PDAC [63]. It has been suggested that dynamic MRI can unmask 80% of the isoattenuating PDACs (Fig. 9) [69]. On the other hand, the most clinically relevant differential diagnoses including focal autoimmune pancreatitis (AIP) and benign focal pancreatic ductal stricture could also be distinguished from isoattenuating PDAC using MRI and PET/CT [70, 71]. In addition to PDAC, a quarter of insulinomas are also isoattenuating on biphasic MDCT [64]. Whole-pancreas CT perfusion, T1-weighted MRI, and quantitative

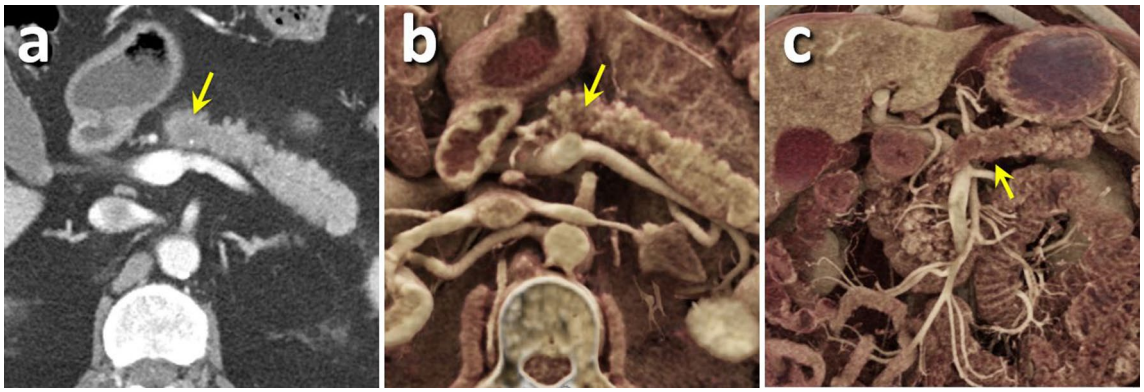

Fig. 10 A 65-year-old male with pancreatic ductal adenocarcinoma. (**a**) Axial, venous phase, post-contrast MDCT image shows subtle isoenhancing mass in the pancreatic neck (yellow arrow). Axial (**b**) and coronal (**b**), venous phase, images with cinematic rendering accentuate focal textural change at the level of the mass (yellow arrows)

assessment of the ADC values have been suggested to be useful to identify pancreatic isoattenuating insulinomas [64, 72].

Subtle pancreatic duct irregularity

Among secondary imaging features of PDAC, we emphasized the importance of irregularities of the main pancreatic duct. The pancreatic duct needs to be carefully evaluated for any subtle contour irregularities, filling defects, or obstructive lesions. Several case reports have documented patients suspected to PDAC who were believed to have normal findings on previous MDCT and MRI, but subtle pancreatic duct irregularity was found in the re-assessment of prior images or endoscopic retrograde cholangiopancreatography (ERCP) [73–75]. From our experience, subtle pancreatic duct irregularity may be best shown on oblique coronal and sagittal MPR CT (and MR) images that optimizes visualization of the pancreatic duct (Fig. 11). Any luminal irregularity or filling defect in the pancreatic duct should be further evaluated with MRCP or endoscopic ultrasound [76].

Diffuse tumor infiltration

Only 5% of PDACs are diffusely infiltrative, but when they are the imaging findings can mimic an inflammatory process such as AIP, as well as pancreatic lymphoma, pancreatoblastoma, and metastasis (Fig. 12) [77]. Although the final diagnosis can be confirmed by clinical history, lab values, and/or tissue sampling, radiologists should be familiar with the main imaging features of these differential diagnoses [77].

Diffuse AIP manifests as diffuse enlargement of the pancreas with delayed enhancement which is known as "sausage-like" gland, the presence of a hypodense ''halo'' surrounding the pancreas, loss of lobular morphology, loss of visualization of the main pancreatic duct, and by the presence of a rim like enhancement in delayed phase (Fig. 13) [77–80]. Lack of main pancreatic duct dilation

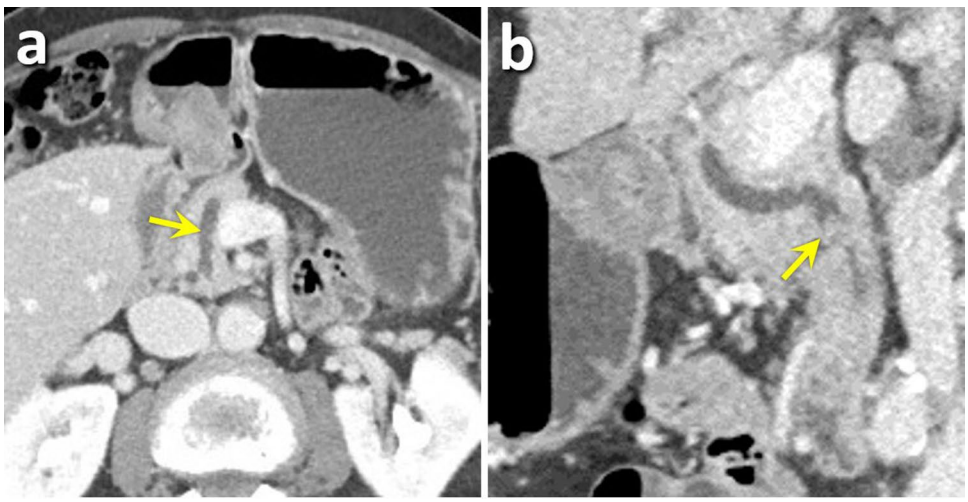

Fig. 11 Axial (**a**) and sagittal oblique (**b**), venous phase, post-contrast MDCT images from an 82-year-old female demonstrate dilated pancreatic duct and subtle pancreatic duct irregularity (yellow arrows). The patient underwent Whipple resection surgery, which confirmed the presence of pancreatic ductal adenocarcinoma (7 mm mass)

can differentiate diffuse AIP from diffuse PDAC [77–80]. In addition, elevated IgG4 levels suggest AIP, but IgG4 can be normal in some AIP patients and normal serum IgG4 does not exclude AIP [81]. As part of both diagnosis and treatment, most AIP patients show excellent response to steroids [82, 83]. The imaging features of focal pancreatitis including focal AIP, acute pancreatitis, and chronic pancreatitis can mimic a focal mass, and the possible interpretation errors are discussed in the next sections.

The second differential diagnosis for diffuse infiltration of the gland is pancreatic lymphoma (Fig. 14) [77, 84, 85]. Several imaging features of diffuse pancreatic lymphoma

Fig. 12 Axial (**a**, **b**) and coronal (**c**), venous phase, post-contrast MDCT images from a 62-year-old female show diffuse heterogeneous enlargement, mild irregular main pancreatic duct dilatation, and severe narrowing superior mesenteric vein. Based on the MDCT findings, pancreatic biopsy was obtained to confirm the diagnosis (potential differential diagnoses: inflammatory process or neoplasm). Histopathological study confirmed the presence of pancreatic ductal adenocarcinoma

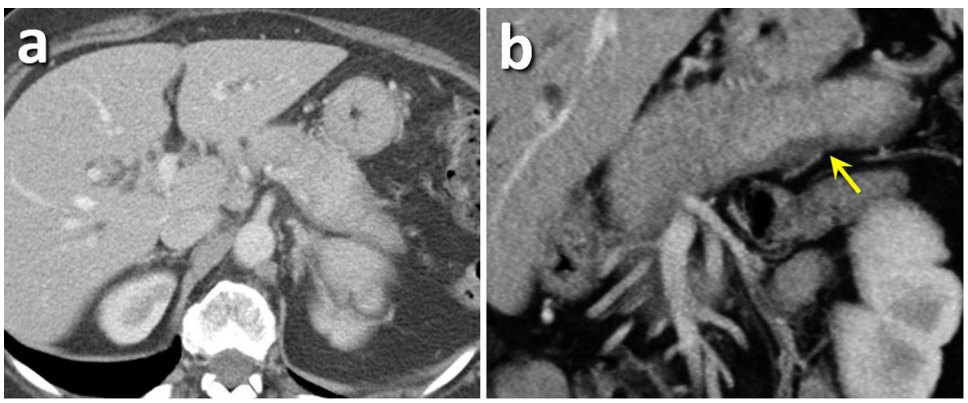

Fig. 13 A 65-year-old female with autoimmune pancreatitis (AIP). Axial (**a**) and coronal (**b**), venous phase, post-contrast MDCT examinations show fusiform sausage-like enlargement of pancreas with peripheral hypoattenuating halo (yellow arrow)

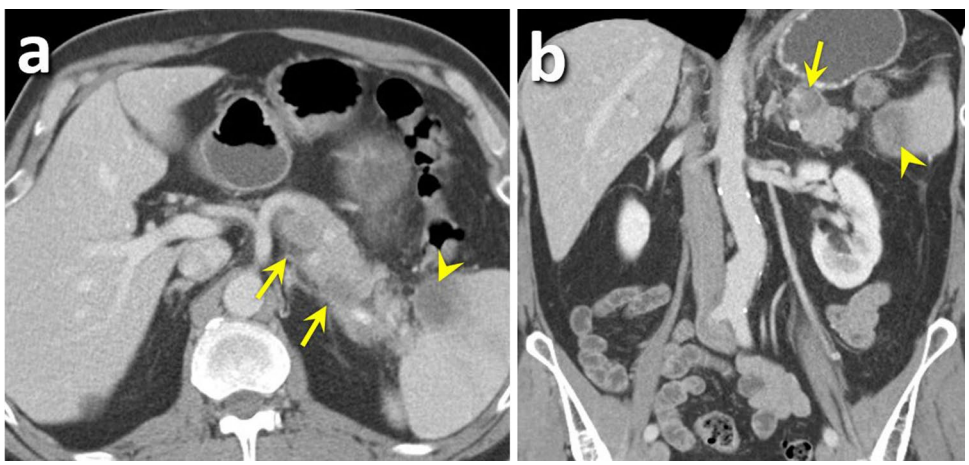

Fig. 14 A 63-year-old male diagnosed with diffuse large B-cell lymphoma with involvement of pancreas and spleen. Axial (**a**) and coronal (**b**), venous phase, post-contrast MDCT examinations show diffuse infiltrative mass throughout pancreatic body and tail (yellow arrows). Lack of pancreatic ductal dilation is against PDAC diagnosis. Presence of splenic lesion (yellow arrowheads) and additional abdominal lymphadenopathy should raise lymphoma as a diagnostic consideration

can be used to distinguish it from PDAC [77, 84]. In general, pancreatic lymphoma is less likely to cause significant main pancreatic duct and common bile duct dilatation compared to PDAC (Fig. 14) [77, 84]. In pancreatic lymphoma, mild common bile duct dilatation is more common than is main pancreatic duct dilatation [77, 84]. Enlarged lymph nodes, infiltration to retroperitoneal or abdominal organs, and invasive tumor growth with loss of anatomic boundaries are also more commonly seen in lymphoma (Fig. 14) [77, 84]. Also, vascular invasion, tumor calcification, and necrosis are less common in pancreatic lymphoma than in PDAC [74, 84]. Considering the better prognosis of pancreatic lymphoma and availability of chemotherapy as an effective treatment, the accurate diagnosis of lymphoma and distinguishing it from PDAC is critical [86].

Metastases to the pancreas are most commonly from cancers of the kidney, lung, breast and colorectal, and from melanoma [87, 88]. Overall, 15–44% of pancreatic metastases have a diffuse morphological pattern [87, 88]. The appearance of pancreatic metastases can be similar to primary PDAC on MDCT [87–89]. Pancreatic metastases often show peripheral or homogeneous (less common) enhancement; while PDACs are generally hypoattenuating lesions [87–89].

Interpretation challenges due to coexisting or underlying pathologies

PDAC in patients with chronic pancreatitis

Differentiation of PDAC from coexisting and/or underlying chronic pancreatitis remains a real challenge (Fig. 15). Chronic pancreatitis is associated with ~ 8-fold increased risk of PDAC within 5 years, and overall 5% of patients with chronic pancreatitis have concurrent PDAC [90]. Therefore, it has been recommended to closely follow-up patients with chronic pancreatitis, even in the first years after diagnosis, to avoid missing coexisting cancer [91].

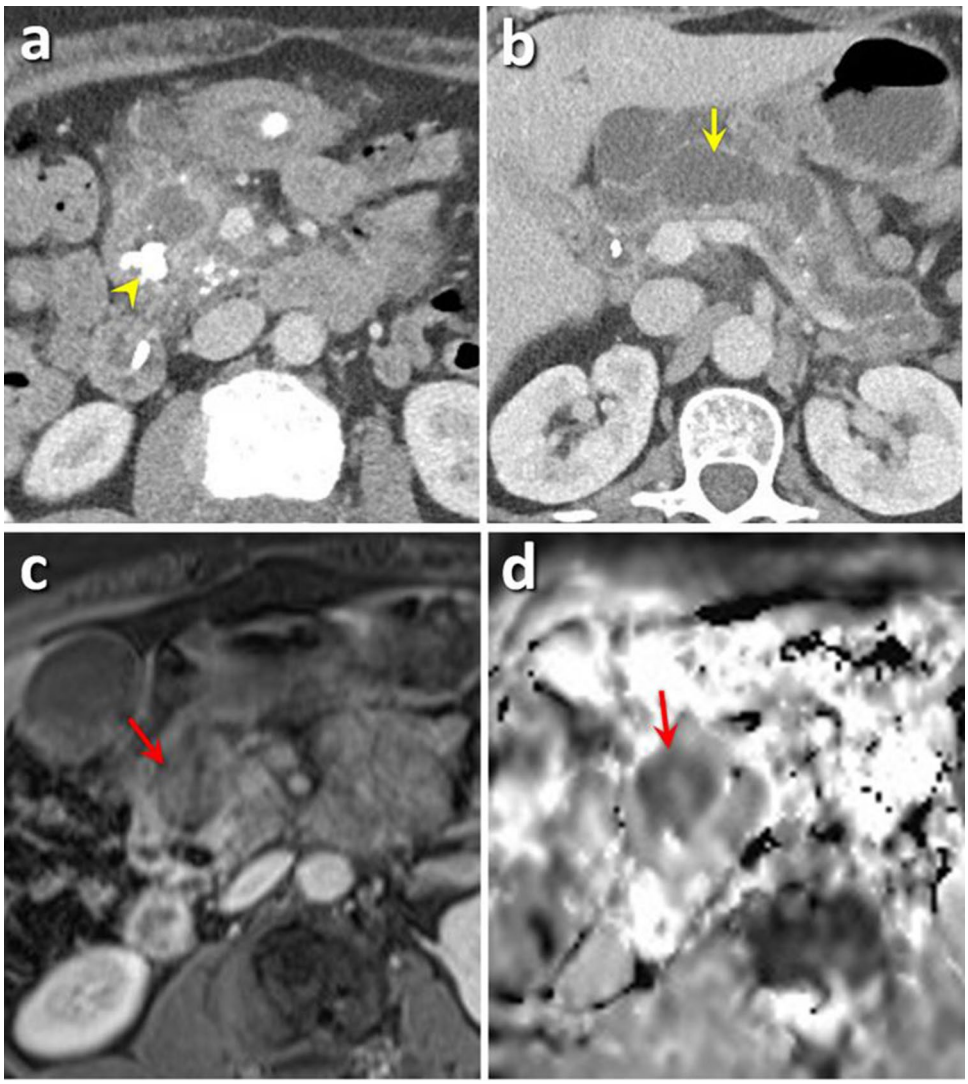

Fig. 15 A 71-year-old female with chronic pancreatitis. Axial (**a**, **b**), venous phase, post-contrast MDCT images show dilated pancreatic duct (yellow arrow) with parenchymal calcifications (yellow arrowhead). Axial post-Gad T1-weighted MR (**c**) and axial DW MR (**d**) images from the same patient show hypoenhancing pancreatic head mass with restricted diffusion (red arrows). Pancreatic biopsy was obtained and the presence of pancreatic ductal adenocarcinoma was pathologically confirmed

In some cases, chronic pancreatitis can form a focal mass mimicking the appearance of PDAC. Furthermore, both chronic pancreatitis and cancer can cause pancreatic duct dilation. Thus, pancreatic ductal dilatation and parenchymal heterogeneity in chronic pancreatitis of the background pancreas can make it difficult to detect a superimposed PDAC (Fig. 15) [92, 93]. The appearance of pancreatic duct dilation may help make this distinction [15, 92, 93]. Abrupt termination of the pancreatic or common bile duct and smooth duct dilatation are more suggestive of a PDAC; whereas irregular duct dilation, diffuse parenchymal calcifications, and parenchymal atrophy favor the presence of chronic pancreatitis [92, 93]. In equivocal cases, other modalities such as PET, MRI (especially DWI sequence), perfusion CT, EUS, and biopsy could be used to establish the diagnosis (Fig. 15) [15, 92–96]. However, none of these methods can be considered as the reference standard and the most sensitive modality for nonsurgical detection of PDAC (in the context of chronic pancreatitis) is EUS-guided biopsy followed by cytopathological examination [97–101].

18FDG-PET can help distinguish PDAC from mass-forming chronic pancreatitis with the pooled sensitivity and specificity of 90% and 84%, respectively [48]. The diagnostic performance of MRI DWI in distinguishing PDAC and mass-forming chronic pancreatitis has been evaluated by a handful of studies with conflicting and inconsistent results [102]. Some reports showed lower ADC values for cancer when compared with pancreatitis, and other reports demonstrated higher or equivalent ADC values [103, 104]. Therefore, DWI is not recommended in routine clinical practice to distinguish cancer from pancreatitis. Perfusion CT is performed by serial image acquisition during contrast injection and its acquired datasets can be assessed using time-attenuation-curve color-coded perfusion maps and semi-quantitative/quantitative analytical methods. It has been shown that perfusion CT driven parameters could help to differentiate mass-mimicking pancreatitis from PDAC [95, 96]. In this regard, studies showed that perfusion CT indices including blood volume (BV), blood flow (BF), mean transit time (MTT), and permeability surface area product (PS) maps could provide sensitivity of 84.6–100% and specificity of 67.9–100% in differentiation between PDAC and mass-mimicking chronic pancreatitis [95, 96]. In comparison with other imaging modalities, EUS and EUS-guided fine needle biopsy are more accurate in establishing the diagnosis of PDAC with the sensitivity and specificity of more than 85% and 95%, respectively [97–101]. Although the sensitivity and specificity of EUS-guided biopsy decrease to 75% in the context of chronic pancreatitis, performing more than seven biopsies using larger needle increases the sensitivity and specificity to > 90% [97–101]. Therefore, any morphologic changes over serial examinations of subjects with chronic pancreatitis may prompt further evaluation with EUS-guided biopsy [97–101].

Distinguishing focal AIP from PDAC can also be very challenging (Fig. 16) [105–107]. Similar methods (i.e., PET, DWI, EUS, and biopsy) can be utilized, as can serum IgG4 levels; however, as noted earlier, normal serum IgG4 does not exclude AIP [81]. Specific imaging features of AIP are also completely discussed earlier.

PDAC arising from intraductal papillary mucinous neoplasm (IPMN)

IPMNs account for 20% of all cystic pancreatic neoplasms and are divided into main-duct, branch-duct, and mixed subtypes [108, 109]. Most IPMNs are incidentally detected on cross-sectional imaging performed for other clinical indications, and it has been estimated that half of the incidentally detected pancreatic cysts are IPMNs [110]. As pre-cancerous

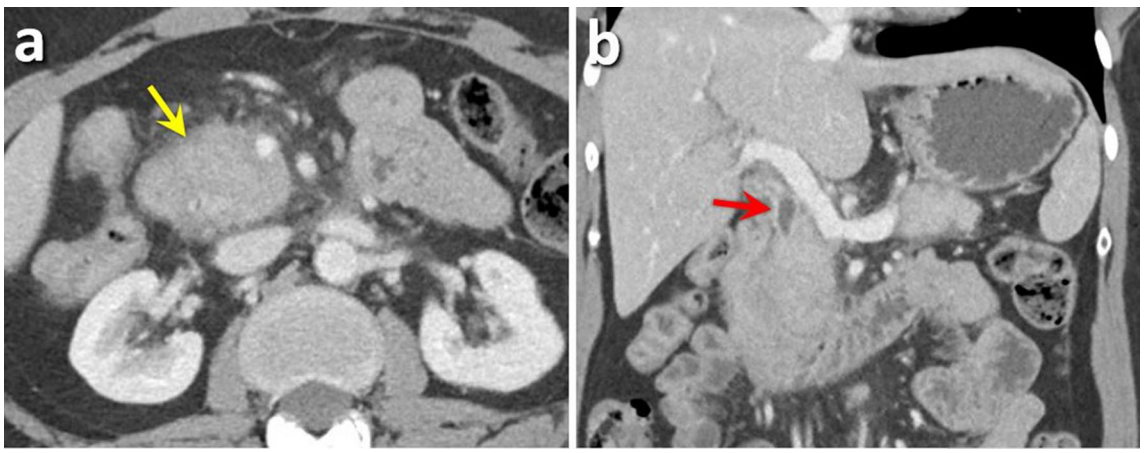

Fig. 16 A 64-year-old female with autoimmune pancreatitis (AIP). Axial (**a**) and coronal (**b**), venous phase, post-contrast MDCT image shows focal enlargement of the pancreatic head (yellow arrow) with mild common bile duct dilatation (red arrow)

lesions, IPMNs can progress to higher grades of dysplasia and to invasive PDAC, which results in the coexisting malignancy rate of 12–68% [108, 111]. In this regard, the precise diagnosis of PDAC arising from IPMN is of importance, since 10% of diagnosed PDACs are related to the underlying IPMNs [110].

Imaging features that may predict malignancy include the presence of enhancing mural nodules, presence of solid focal components, cyst size of ≥ 3 cm, main pancreatic duct dilatation (especially caliber of ≥ 10 mm), thick/enhanced wall and/or septum (Fig. 17) [112, 113]. Guidelines recommended surgical resection for all symptomatic IPMNs, asymptomatic main-duct and mixed IPMNs, and branch-duct IPMNs with high-risk features [114–116]. Asymptomatic branch-duct IPMNs without high-risk features are usually followed using serial exams [114]. Although MDCT and MRI are traditionally used for these serial assessments, the solid components of IPMNs and superimposed PDACs can be difficult to detect on non-contrast MRI and MDCT [110, 117]. At our institution, MRCP is routinely performed with IV contrast to facilitate detection of a solid component or synchronous PDAC. It has been suggested that MRCP as a reliable and noninvasive method, possess higher diagnostic performance in visualizing subtle changes and complex cystic mass related to the branch-duct IPMN [114, 118–120]. Other diagnostic modalities including MDCT, MRI, ERCP, EUS, and 18FDG-PET/CT can also be used to serially evaluate branch-duct IPMNs [121–124]. The presence of an enhancing solid component and other "high-risk stigma" should prompt further evaluation with EUS and/or biopsy; high-risk patients should undergo surgical resection based on the results of the EUS and biopsy [110, 114].

Interpretation challenges due to cognitive errors

Distracting findings

Distraction errors include reader fatigue, interruptions to look at other cases, phone calls, etc. Among all these causes, satisfaction of search has been considered as one of the leading causes of interpretation errors [125]. Satisfaction of search, also known as premature closure, is defined when identifying initial abnormality on an image halts searching and result in prematurely ended examination and therefore other abnormalities are missed [126, 127]. In the context of multiple-target search (e.g., MDCT of the pancreas), the goal is to detect all targets using a detailed search termination rule [128]. As it was mentioned earlier, PDAC may coexist or arise from underlying IPMNs and pancreatitis. IPMNs and other cystic lesions are easy to detect due to the relatively large difference in signal compared to background pancreas (Figs. 18–19). Radiologists can be distracted by these cystic lesions and fail to detect the subtle synchronous PDAC (Figs. 18–19).

Incidental findings

Pancreatic pathologies may be present on examinations obtained for other clinical indications. The radiologists may be focusing most of his or her energy searching for pathologies in other organs and pay relatively less attention to the pancreas. At our institution, approximately 6% of PDAC patients who underwent surgical resection presented with an incidental pancreatic mass [129]. In another report, 30% of patients with incidentally diagnosed pancreatic mass were diagnosed with PDAC [130]. Furthermore, pancreatic cysts are incidentally detected in 2.6–19.6% of abdominal cross-sectional imaging, and more than half of PanNETs are identified incidentally [131–134]. In such cases, accurate diagnosis of cancer is challenging due to the suboptimal protocol or

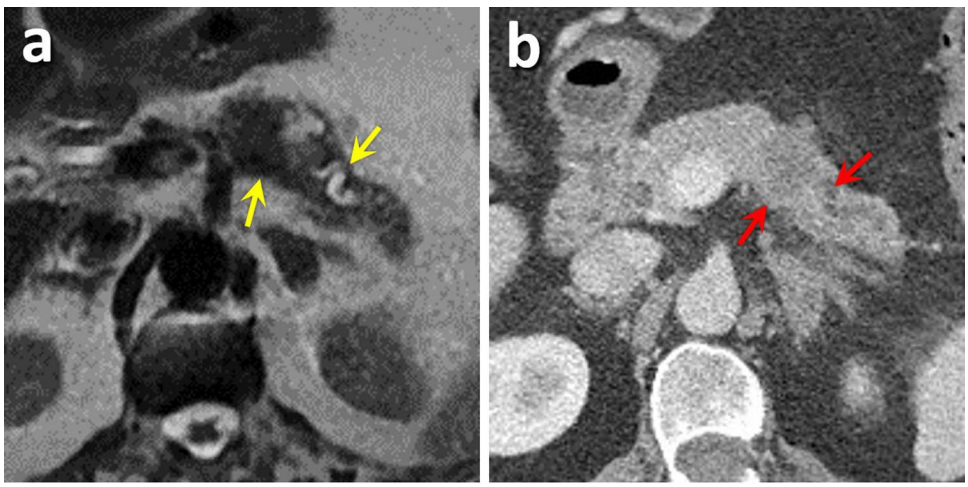

Fig. 17 A 71-year-old female referred from the outside institution for intraductal papillary mucinous neoplasm (IPMN) which was diagnosed based on MRI findings. The solid component with intermediate T2-weighted MR image (**a**) was not appreciated at the outside exam (yellow arrows). The patient was assessed using MDCT; venous phase of axial contrast-enhanced MDCT image (**b**) reveals solid and cystic mass due to a pancreatic ductal adenocarcinoma arising from the IPMN (red arrows)

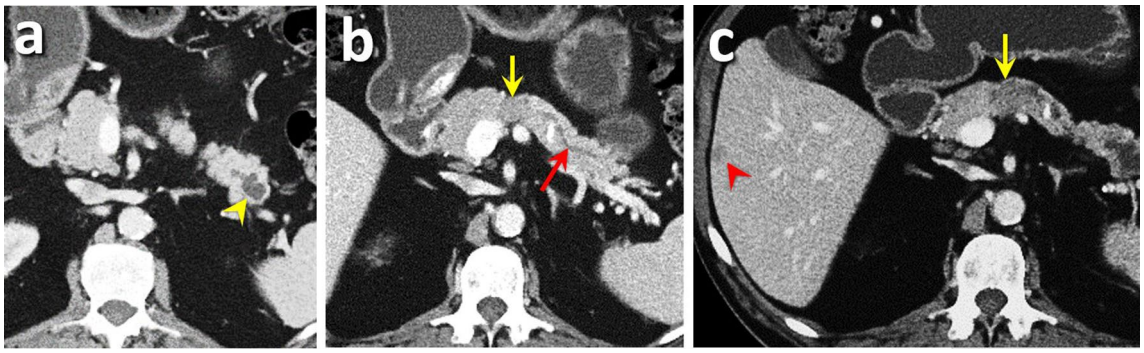

Fig. 18 A 68-year-old man who presented for evaluation of intraductal papillary mucinous neoplasm (IPMN). **a**, **b** Axial, venous phase, contrast-enhanced MDCT images show IPMN in the pancreatic tail. Subtle hypoenhancing mass (yellow arrows) was also detected in the pancreatic body in addition to a cystic mass in the pancreatic tail (yellow arrowhead) and pancreatic duct dilation (red arrow). **c** After 6-months, follow-up axial, venous phase, contrast-enhanced MDCT image demonstrates metastatic pancreatic ductal adenocarcinoma with liver metastases (red arrowhead)

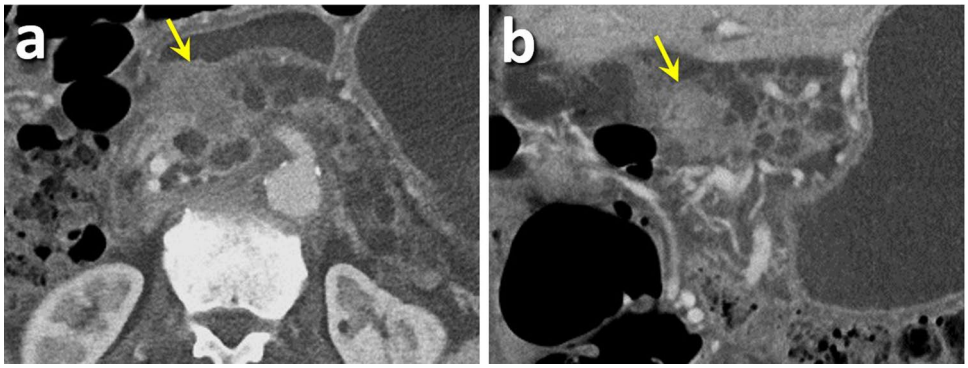

Fig. 19 Axial (**a**) and coronal (**b**), venous phase, post-contrast MDCT images from a 73-year-old man with multifocal intraductal papillary mucinous neoplasms (IPMNs) show a subtle solid enhancing mass in the pancreatic head (yellow arrows) that has a different appearance than background IPMNs. The patient underwent biopsy and the presence of pancreatic ductal adenocarcinoma was pathologically confirmed

"edge-of-film" effect. Therefore, systematic evaluation of all organs within the field of view is essential, and all incidental pancreatic masses should be precisely assessed using biphasic MDCT protocol with an optimal field of view [112].

Interpretation challenges due to mimickers of PDAC

Focal fatty infiltration

Focal fatty infiltration is a relatively common finding in the adult population, especially in old or obese subjects [135]. Focal fatty infiltration is most prominent in the anterior aspect of the pancreatic head and uncinate process, while the posterior aspect is usually spared. There is also sparing of the ventral anlage, which forms the caudal portion of the pancreatic head and uncinate process, due to paucity of fat cells [135]. If fatty infiltration contains a sufficient amount of fat, it can be detected on non-contrast MDCT by measuring fat attenuation units. However, in the case of insufficient fat, the lesion may not show significant fat attenuation and can mimic PDAC on MDCT (Fig. 20) [135]. In these instances, the absence of mass effect on the common bile duct and pancreatic duct, ductal dilation, abnormal pancreatic contour, abnormal pancreatic parenchyma, and vessel displacement can be used to differentiate focal fatty infiltration from PDAC [135, 136]. The characteristic fat signal on MRI can confirm the diagnosis and differentiate focal fatty infiltration from PDAC (Fig. 20) [135, 137, 138].

Intrapancreatic accessory spleen (IPAS)

Failure of the fusion of splenic anlage in the dorsal mesogastrium results in accessory spleens during embryogenesis [139]. It has been reported that up to one-third of patients have an IPAS in postmortem autopsies [140]. However, these lesions are rarely detected on a routine MDCT due to their small size and the limited resolution of conventional imaging modalities [141]. IPAS may mimic PanNET, and

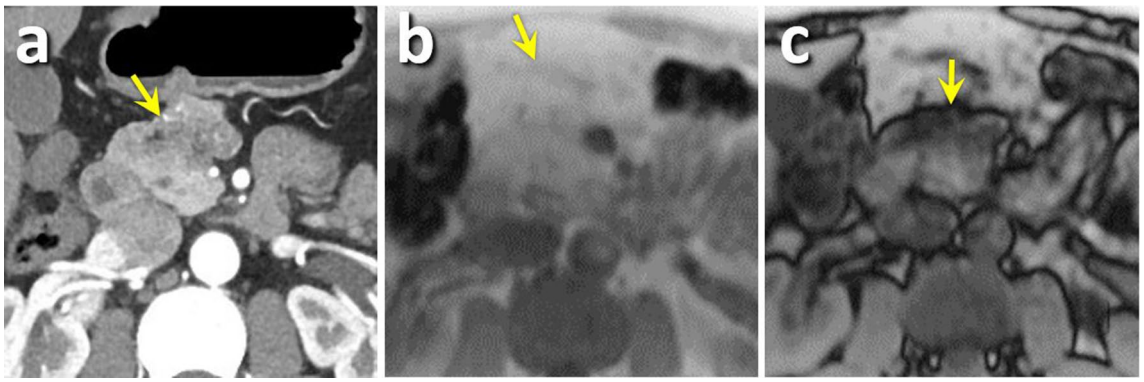

Fig. 20 Axial, venous phase, post-contrast MDCT image (**a**), axial in-phase (**b**) and axial out-of-phase (**c**) MR images from a 39-year-old man show focal fatty infiltration of the pancreas (yellow arrows)

hypervascular metastases on MDCT; so, it can be considered as a potential source of interpretation errors [141–143].

IPAS should mirror splenic attenuation and signal on all MDCT phases and MRI sequences (Fig. 21) [141–143]. Since the attenuation of the spleen is higher in comparison with the pancreas, IPAS can be easily detected during all phases of biphasic MDCT [141–143]. Similarly, IPAS shows lower signal on T1-weighted MRI and higher signal on T2-weighted MRI [141–143]. Furthermore, IPAS usually located at the tip or along the dorsal surface of the pancreatic tail [143]. Other imaging characteristics and methods including arciform splenic enhancement pattern in arterial phase, super-paramagnetic iron oxide-enhanced MRI, technetium 99m (Tc-99m) heat-damaged red blood cell scintigraphy, and Tc-99m sulfur colloid scintigraphy [144] can also be obtained to confirm the diagnosis when IPAS suspected [143, 145, 146].

Pancreatitis

Inflammatory soft-tissue infiltration and parenchymal heterogeneity in the setting of pancreatitis can mimic PDAC. All types of pancreatitis, including acute and chronic pancreatitis as well as AIP can mimic PDAC. Due to the high rate of co-occurrence between these conditions and possible causal relationships between pancreatitis and PDAC, radiologists should be familiar with the distinct imaging features of acute/chronic pancreatitis (Fig. 22) and focal/diffuse AIP, to distinguish them from PDAC (described in prior sections). In this regard, it has been suggested that the risk of PDAC is ~ 10 times higher in patients with a primary episode of acute pancreatitis, especially in patients who develop chronic pancreatitis [147]. Acute pancreatitis can also be the first presentation of underlying PDAC [147]. As such, imaging follow-up and screening are important to exclude underlying PDACs after an episode of acute pancreatitis, and radiologists should be able to detect PDAC in the context of pancreatitis.

Fig. 21 Arterial (**a**) and venous (**b**) phase of axial contrast-enhanced MDCT from a 79-year-old man show intrapancreatic accessory spleen (IPAS) (yellow arrows). IPAS mimics pancreatic ductal adenocarcinoma and pancreatic neuroendocrine tumors. Enhancement of the mass is same as spleen on both arterial and venous phase, which confirms the diagnosis of IPAS

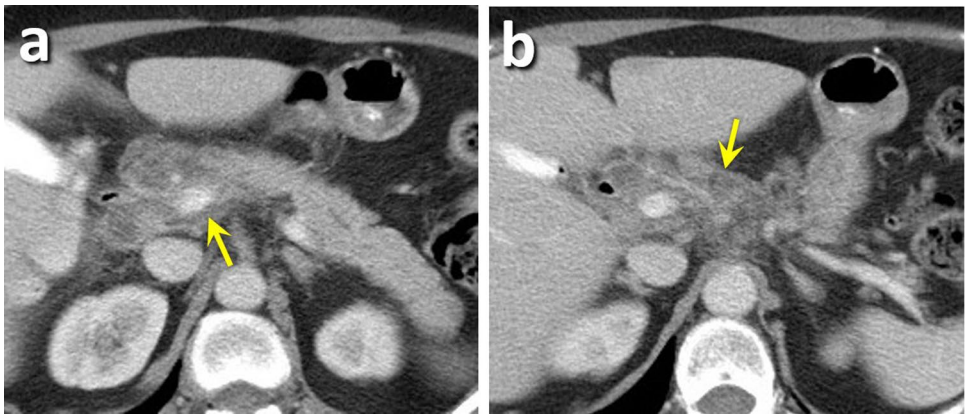

Fig. 22 **a**, **b** Venous phase of axial contrast-enhanced MDCT images from a 79-year-old woman with acute pancreatitis. Presence of infiltrative soft tissue (yellow arrows) arouses suspicion of malignancy. Pancreatic biopsy was obtained which showed no evidence of malignancy, and MDCT findings resolved on follow-up images 2-years later

Conclusion

MDCT is one of the most commonly used imaging modalities for the initial evaluation of suspected PDAC. Several pitfalls are associated with diagnoses of PDAC using MDCT. Optimal imaging technique is key to the detection of subtle cases, and errors in each step of image acquisition carry a potential for contributing to misdiagnosis. Accurate diagnosis requires familiarity with a variety of factors that can lead to interpretation errors. Detection of PDAC can be challenging due to intrinsic tumor features and presence of coexisting pathology that can distract the radiologist from the more subtle lesions. Normal structures and non-neoplastic diseases can also mimic the imaging appearance of PDAC. Recognition and mitigation of such technical and interpretation errors can help early PDAC diagnosis and improve patient prognosis.

Funding No funding was received for this study.

Compliance with ethical standards

Conflict of interest The authors declare that they have no relevant conflict of interest.

Ethical approval All procedures performed in this study were in accordance with the ethical standards of the institutional and/or national research committee and with the 1964 Helsinki Declaration and its later amendments or comparable ethical standards.

References

1. Jemal A, Siegel R, Ward E, et al (2006) Cancer statistics, 2006. CA Cancer J Clin. 56 (2):106-130.
2. SEER Cancer Statistics Review, 1975–2014. National Cancer Institute, 2019. Available at: https://seer.cancer.gov/csr/1975_2014/). Accessed August 23, 2019.
3. Fitzmaurice C, Dicker D, Pain A, et al (2015) The global burden of cancer 2013. JAMA Oncol. 1 (4):505-527.
4. Bray F, Ferlay J, Soerjomataram I, et al (2018) Global cancer statistics 2018: GLOBOCAN estimates of incidence and mortality worldwide for 36 cancers in 185 countries. CA Cancer J Clin. 68 (6):394-424.
5. Gong J, Tuli R, Shinde A, Hendifar AE (2016) Meta-analyses of treatment standards for pancreatic cancer. Mol Clin Oncol. 4(3):315-325.
6. Evans DB, Farnell MB, Lillemoe KD, et al (2009) Surgical treatment of resectable and borderline resectable pancreas cancer: expert consensus statement. Ann Surg Onco. 16(7):1736-1744.
7. Ryan DP, Hong TS, Bardeesy N (2014) Pancreatic adenocarcinoma. N Engl J Med. 371(11):1039-1049.
8. Wray CJ, Ahmad SA, Matthews JB, Lowy AM (2005) Surgery for pancreatic cancer: recent controversies and current practice. Gastroenterology. 128 (6):1626-1641.
9. Howlader N, Noone A, Krapcho M, et al (2017) SEER cancer statistics review, 1975–2014. Bethesda, MD: National Cancer Institute 2018.
10. Al-Hawary MM, Francis IR, Chari ST, et al (2014) Pancreatic ductal adenocarcinoma radiology reporting template: consensus statement of the Society of Abdominal Radiology and the American Pancreatic Association. Radiology. 270 (1):248-260.
11. National Comprehensive Cancer Network (2011) NCCN clinical practice guidelines in oncology (NCCN guidelines). Central Nervous System Cancers Version 2. 19-21.
12. Chu LC, Goggins MG, Fishman EK (2017) Diagnosis and detection of pancreatic cancer. Cancer J. 23 (6):333-342.
13. Toft J, Hadden WJ, Laurence JM, et al (2017) Imaging modalities in the diagnosis of pancreatic adenocarcinoma: A systematic review and meta-analysis of sensitivity, specificity and diagnostic accuracy. Eur J Radiol. 92:17-23.
14. Raman SP, Horton KM, Fishman EK (2012) Multimodality imaging of pancreatic cancer—computed tomography, magnetic resonance imaging, and positron emission tomography. Cancer J. 18 (6):511-522.
15. Horton KM, Fishman EK (2002) Adenocarcinoma of the pancreas: CT imaging. Radiol Clin North Am. 40 (6):1263-1272.
16. Pawlik TM, Laheru D, Hruban RH, et al (2008) Evaluating the impact of a single-day multidisciplinary clinic on the management of pancreatic cancer. Ann Surg Oncol. 15 (8):2081-2088.
17. Gonoi W, Hayashi TY, Okuma H, et al (2017) Development of pancreatic cancer is predictable well in advance using contrast-enhanced CT: a case–cohort study. Eur Radiol. 27 (12):4941-4950.
18. CTisus (2019) Educational Tools. Available at: https://www.ctisus.com/responsive/protocols. Accessed August 23, 2019.
19. Brennan DD, Zamboni GA, Raptopoulos VD, Kruskal JB (2007) Comprehensive preoperative assessment of pancreatic

adenocarcinoma with 64-section volumetric CT. Radiographics. 27 (6):1653-1666.
20. Somers I, Bipat S (2017) Contrast-enhanced CT in determining resectability in patients with pancreatic carcinoma: a meta-analysis of the positive predictive values of CT. Eur Radio. 27 (8):3408-3435.
21. Megibow AJ, Zhou XH, Rotterdam H, et al (1995) Pancreatic adenocarcinoma: CT versus MR imaging in the evaluation of resectability–report of the Radiology Diagnostic Oncology Group. Radiology. 195 (2):327-332.
22. Soriano A, Castells A, Ayuso C, et al (2004) Preoperative staging and tumor resectability assessment of pancreatic cancer: prospective study comparing endoscopic ultrasonography, helical computed tomography, magnetic resonance imaging, and angiography. Am J Gastroenterol. 99 (3):492-501.
23. Fishman EK, Ney DR, Heath DG, et al (2006) Volume rendering versus maximum intensity projection in CT angiography: what works best, when, and why. Radiographics. 26 (3):905-922.
24. Nino-Murcia M, Jeffrey Jr RB, Beaulieu CF, Li KC, Rubin GD (2001) Multidetector CT of the pancreas and bile duct system: value of curved planar reformations. AJR Am J Roentgenol. 176 (3):689-693.
25. Grieser C, Steffen IG, Grajewski L, et al (2010) Preoperative multidetector row computed tomography for evaluation and assessment of resection criteria in patients with pancreatic masses. Acta Radiol. 51 (10):1067-1077.
26. Fang C-h, Zhu W, Wang H, et al (2012) A new approach for evaluating the resectability of pancreatic and periampullary neoplasms. Pancreatology. 12 (4):364-371.
27. Catalano C, Laghi A, Fraioli F, et al (2003) Pancreatic carcinoma: the role of high-resolution multislice spiral CT in the diagnosis and assessment of resectability. Eur Radiol. 13 (1):149-156.
28. Yang R, Lu M, Qian X, et al (2014) Diagnostic accuracy of EUS and CT of vascular invasion in pancreatic cancer: a systematic review. J Cancer Res Clin Oncol. 140 (12):2077-2086.
29. Chu LC, Johnson PT, Fishman EK (2018) Cinematic rendering of pancreatic neoplasms: preliminary observations and opportunities. Abdom Radiol (NY). 43 (11):3009-3015.
30. Johnson PT, Schneider R, Lugo-Fagundo C, Johnson MB, Fishman EK (2017) MDCT angiography with 3D rendering: a novel cinematic rendering algorithm for enhanced anatomic detail. AJR Am J Roentgenol. 209 (2):309-312.
31. Gillies RJ, Kinahan PE, Hricak H (2015) Radiomics: images are more than pictures, they are data. Radiology. 278 (2):563-577.
32. Chu LC, Park S, Kawamoto S, et al (2019) Utility of CT Radiomics Features in Differentiation of Pancreatic Ductal Adenocarcinoma From Normal Pancreatic Tissue. AJR Am J Roentgenol. 213(2):349-357.
33. Chen F-M, Ni J-M, Zhang Z-Y, et al (2016) Presurgical evaluation of pancreatic cancer: a comprehensive imaging comparison of CT versus MRI. AJR Am J Roentgenol. 206 (3):526-535.
34. Sheridan M, Ward J, Guthrie J, et al (1999) Dynamic contrast-enhanced MR imaging and dual-phase helical CT in the preoperative assessment of suspected pancreatic cancer: a comparative study with receiver operating characteristic analysis. AJR Am J Roentgenol. 173 (3):583-590.
35. Erturk SM, Ichikawa T, Sou H, et al (2006) Pancreatic adenocarcinoma: MDCT versus MRI in the detection and assessment of locoregional extension. J Comput Assist Tomogr. 30 (4):583-590.
36. Bipat S, Phoa SSS, van Delden OM, et al (2005) Ultrasonography, computed tomography and magnetic resonance imaging for diagnosis and determining resectability of pancreatic adenocarcinoma: a meta-analysis. J Comput Assist Tomogr. 29 (4):438-445.
37. Ito T, Sugiura T, Okamura Y, et al (2017) The diagnostic advantage of EOB-MR imaging over CT in the detection of liver metastasis in patients with potentially resectable pancreatic cancer. Pancreatology. 17 (3):451-456.
38. Motosugi U, Ichikawa T, Morisaka H, et al (2011) Detection of pancreatic carcinoma and liver metastases with Gadoxetic acid–enhanced MR imaging: comparison with contrast-enhanced multi–detector row CT. Radiology. 260 (2):446-453.
39. Lens E, Gurney-Champion OJ, Tekelenburg DR, et al (2016) Abdominal organ motion during inhalation and exhalation breath-holds: pancreatic motion at different lung volumes compared. Radiother Oncol. 121 (2):268-275.
40. Schultz CL, Alfidi R, Nelson AD, Kopiwoda SY, Clampitt ME (1984) The effect of motion on two-dimensional Fourier transformation magnetic resonance images. Radiology. 152 (1):117-121.
41. Wood ML, Henkelman RM (1985) MR image artifacts from periodic motion. Med Phys. 12 (2):143-151.
42. Simeone J, Edelman R, Stark D, et al (1985) Surface coil MR imaging of abdominal viscera. Part III. The pancreas. Radiology. 157 (2):437-441.
43. Yang RK, Roth CG, Ward RJ, deJesus JO, Mitchell DG (2010) Optimizing abdominal MR imaging: approaches to common problems. Radiographics. 30 (1):185-199.
44. Wood ML, Runge V, Henkelman RM (1988) Overcoming motion in abdominal MR imaging. AJR Am J Roentgenol. 150 (3):513-522.
45. Patel BN (2018) Routine MR Imaging for Pancreas. Magn Reson Imaging Clin N Am. 26 (3):315-322.
46. Canellas R, Rosenkrantz AB, Taouli B, et al (2019) Abbreviated MRI Protocols for the Abdomen. Radiographics. 39(3):744-758.
47. Orlando L, Kulasingam S, Matchar DB (2004) Meta-analysis: the detection of pancreatic malignancy with positron emission tomography. Aliment Pharmacol Ther. 20 (10):1063-1070.
48. Rijkers A, Valkema R, Duivenvoorden H, Van Eijck CH (2014) Usefulness of F-18-fluorodeoxyglucose positron emission tomography to confirm suspected pancreatic cancer: a meta-analysis. Eur J Surg Oncol. 40 (7):794-804.
49. Yukutake M, Sasaki T, Serikawa M, et al (2014) The effect of respiratory-gated positron emission tomography/computed tomography in patients with pancreatic cancer. Hell J Nucl Med. 17 (1):31-36.
50. Tsuchiya R, Noda T, Harada N, et al (1986) Collective review of small carcinomas of the pancreas. Ann Surg. 203 (1):77.
51. Egawa S, Takeda K, Fukuyama S, et al (2004) Clinicopathological aspects of small pancreatic cancer. Pancreas. 28 (3):235-240.
52. Bronstein YL, Loyer EM, Kaur H, et al (2004) Detection of small pancreatic tumors with multiphasic helical CT. AJR Am J Roentgenol. 182 (3):619-623.
53. Ichikawa T, Haradome H, Hachiya J, et al (1997) Pancreatic ductal adenocarcinoma: preoperative assessment with helical CT versus dynamic MR imaging. Radiology. 202 (3):655-662.
54. Yoon SH, Lee JM, Cho JY, et al (2011) Small (≤ 20 mm) pancreatic adenocarcinomas: analysis of enhancement patterns and secondary signs with multiphasic multidetector CT. Radiology. 259 (2):442-452.
55. Ahn SS, Kim M-J, Choi J-Y, et al (2009) Indicative findings of pancreatic cancer in prediagnostic CT. Eur Radiol. 19 (10):2448-2455.
56. Tamada T, Ito K, Kanomata N, et al (2016) Pancreatic adenocarcinomas without secondary signs on multiphasic multidetector CT: association with clinical and histopathologic features. Eur Radiol. 26 (3):646-655.
57. Yoshinobu T, Abe K, Sasaki Y, et al (2011) Data management solution for large-volume computed tomography in an existing picture archiving and communication system (PACS). J Digit Imaging. 24(1):107-113.
58. Guchlerner L, Wichmann JL, Tischendorf P, et al (2018) Comparison of thick- and thin-slice images in thoracoabdominal

trauma CT: a retrospective analysis. Eur J Trauma Emerg Surg. Sep 28.
59. Woo HS, Kim KJ, Kim TJ, et al (2007) JPEG 2000 compression of abdominal CT: difference in tolerance between thin-and thick-section images. AJR Am J Roentgenol. 189(3):535-541.
60. Ding Y, Zhou J, Sun H, et al (2013) Contrast-enhanced multiphasic CT and MRI findings of adenosquamous carcinoma of the pancreas. Clin Imaging. 37 (6):1054-1060.
61. Tatli S, Mortele KJ, Levy AD, et al (2005) CT and MRI features of pure acinar cell carcinoma of the pancreas in adults. AJR Am J Roentgenol. 184 (2):511-519.
62. Kim WH, Lee JY, Park HS, et al (2013) Lymphoepithelial cyst of the pancreas: comparison of CT findings with other pancreatic cystic lesions. Abdom Imaging. 38 (2):324-330.
63. Kim JH, Park SH, Yu ES, et al (2010) Visually isoattenuating pancreatic adenocarcinoma at dynamic-enhanced CT: frequency, clinical and pathologic characteristics, and diagnosis at imaging examinations. Radiology. 257 (1):87-96.
64. Zhu L, Xue H-d, Sun H, et al (2016) Isoattenuating insulinomas at biphasic contrast-enhanced CT: frequency, clinicopathologic features and perfusion characteristics. Eur Radiol. 26 (10):3697-3705.
65. Fletcher JG, Wiersema MJ, Farrell MA, et al (2003) Pancreatic malignancy: value of arterial, pancreatic, and hepatic phase imaging with multi–detector row CT. Radiology. 229 (1):81-90.
66. Prokesch RW, Chow LC, Beaulieu CF, Bammer R, Jeffrey Jr (2002) Isoattenuating pancreatic adenocarcinoma at multi–detector row CT: secondary signs. Radiology. 224 (3):764-768.
67. Scialpi M, Pierotti L, Piscioli I, et al (2012) Detection of small (<= 20 mm) pancreatic adenocarcinoma: histologic grading and CT enhancement features. Radiology. 262 (3):1044-1045; author reply 1045.
68. Ishigami K, Yoshimitsu K, Irie H, et al (2009) Diagnostic value of the delayed phase image for iso-attenuating pancreatic carcinomas in the pancreatic parenchymal phase on multidetector computed tomography. Eur J Radiol. 69 (1):139-146.
69. Blouhos K, Boulas K, Tsalis K, Hatzigeorgiadis AJSo (2015) The isoattenuating pancreatic adenocarcinoma: review of the literature and critical analysis. Surg Oncol. 24 (4):322-328.
70. Shanbhogue AKP, Tirumani SH, Prasad SR, Fasih N, McInnes M (2011) Benign biliary strictures: a current comprehensive clinical and imaging review. AJR Am J Roentgenol. 197 (2):295-306.
71. Fritz S, Bergmann F, Grenacher L, et al (2014) Diagnosis and treatment of autoimmune pancreatitis types 1 and 2. Br J Surg. 101 (10):1257-1265.
72. Shi Z, Li X, You R, et al (2018) Homogenously isoattenuating insulinoma on biphasic contrast-enhanced computed tomography: Little benefits of diffusion-weighted imaging for lesion detection. Oncol Lett. 16 (3):3117-3125.
73. Ochi K, Hasuoka H, Mizushima T, Matsumura N, Harada H (1998) A case of small pancreatic cancer diagnosed by serial follow-up studies promptly by a positive K-ras point mutation in pure pancreatic juice. Am J Gastroenterol. 93 (8):1366.
74. Fujisaki S, Takashina M, Tomita R, et al (2016) Two Cases Pancreatic Carcinoma Detected Incidentally during Treatment of Acute Abdomen from Other Causes. Gan To Kagaku Ryoho. 43 (12):1662-1664.
75. Blouhos K, Boulas KA, Tselios DG, et al (2013) Surgically proved visually isoattenuating pancreatic adenocarcinoma undetected in both dynamic CT and MRI. Was blind pancreaticoduodenectomy justified? Int J Surg Case Rep. 4 (5):466-469.
76. Hanada K, Okazaki A, Hirano N, et al (2015) Effective screening for early diagnosis of pancreatic cancer. Best Pract Res Clin Gastroenterol. 29 (6):929-939.
77. Low G, Panu A, Millo N, Leen E (2011) Multimodality imaging of neoplastic and nonneoplastic solid lesions of the pancreas. Radiographics. 31 (4):993-1015.
78. Chang WI, Kim BJ, Lee JK, et al (2009) The clinical and radiological characteristics of focal mass-forming autoimmune pancreatitis: comparison with chronic pancreatitis and pancreatic cancer. Pancreas. 38 (4):401-408.
79. Hafezi-Nejad N, Singh VK, Fung C, Takahashi N, Zaheer AJMRIC (2018) MR Imaging of Autoimmune Pancreatitis. Magn Reson Imaging Clin N Am. 26 (3):463-478.
80. Irie H, Honda H, Baba S, et al (1998) Autoimmune pancreatitis: CT and MR characteristics. AJR Am J Roentgenol. 170 (5):1323-1327.
81. Katabathina VS, Khalil S, Shin S, et al (2016) Immunoglobulin G4–Related Disease: Recent Advances in Pathogenesis and Imaging Findings. Radiol Clin North Am. 54 (3):535-551.
82. Chari ST, Smyrk TC, Levy MJ, et al (2006) Diagnosis of autoimmune pancreatitis: the Mayo Clinic experience. Clin Gastroenterol Hepatol. 4 (8):1010-1016.
83. Church NI, Pereira SP, Deheragoda MG, et al (2007) Autoimmune pancreatitis: clinical and radiological features and objective response to steroid therapy in a UK series. Am J Gastroenterol. 102 (11):2417.
84. Merkle EM, Bender GN, Brambs HJ (2000) Imaging findings in pancreatic lymphoma: differential aspects. AJR Am J Roentgenol. 174 (3):671-675.
85. Ishigami K, Tajima T, Nishie A, et al (2010) MRI findings of pancreatic lymphoma and autoimmune pancreatitis: a comparative study. Eur J Radiol. 74 (3):22-28.
86. Tuchek J, De SJ, Pickleman J (1993) Diagnosis, surgical intervention, and prognosis of primary pancreatic lymphoma. Am Surg. 59 (8):513-518.
87. Tsitouridis I, Diamantopoulou A, Michaelides M, et al (2010) Pancreatic metastases: CT and MRI findings. Diagn Interv Radiol. 16 (1):45.
88. Kelekis NL, Semelka RC, Siegelman ES (1996) MRI of pancreatic metastases from renal cancer. J Comput Assist Tomogr. 20 (2):249-253.
89. Klein KA, Stephens DH, Welch TJ (1998) CT characteristics of metastatic disease of the pancreas. Radiographics. 18 (2):369-378.
90. Narkhede RA, Desai GS, Prasad PP, Wagle PK (2019) Diagnosis and Management of Pancreatic Adenocarcinoma in the Background of Chronic Pancreatitis: Core Issues. Dig Dis. 37(4):315-324.
91. Kirkegård J, Mortensen FV, Cronin-Fenton D (2017) Chronic pancreatitis and pancreatic cancer risk: a systematic review and meta-analysis. Am J Gastroenterol. 112 (9):1366.
92. Karasawa E, Goldberg HI, Moss AA, Federle M, London SS (1983) CT pancreatogram in carcinoma of the pancreas and chronic pancreatitis. Radiology. 148 (2):489-493.
93. Yin Q, Zou X, Zai X, et al (2015) Pancreatic ductal adenocarcinoma and chronic mass-forming pancreatitis: Differentiation with dual-energy MDCT in spectral imaging mode. Eur J Radiol. 84 (12):2470-2476.
94. Prokesch RW, Schima W, Chow LC, Jeffrey RB (2003) Multidetector CT of pancreatic adenocarcinoma: diagnostic advances and therapeutic relevance. Eur Radiol. 13 (9):2147-2154.
95. Yadav AK, Sharma R, Kandasamy D, et al (2016) Perfusion CT - Can it resolve the pancreatic carcinoma versus mass forming chronic pancreatitis conundrum? Pancreatology. 16(6):979-987.
96. Aslan S, Nural MS, Camlidag I, et al (2019) Efficacy of perfusion CT in differentiating of pancreatic ductal adenocarcinoma from mass-forming chronic pancreatitis and characterization of isoattenuating pancreatic lesions. Abdom Radiol (NY). 44(2):593-603.

97. Fritscher-Ravens A, Brand L, Knöfel WT, et al (2002) Comparison of endoscopic ultrasound-guided fine needle aspiration for focal pancreatic lesions in patients with normal parenchyma and chronic pancreatitis. Am J Gastroenterol. 97 (11):2768.
98. Varadarajulu S, Tamhane A, Eloubeidi MA (2005) Yield of EUS-guided FNA of pancreatic masses in the presence or the absence of chronic pancreatitis. Gastrointest Endosc. 62 (5):728-736.
99. Bang JY, Varadarajulu S (2014) Neoplasia in chronic pancreatitis: how to maximize the yield of endoscopic ultrasound-guided fine needle aspiration. Clin Endosc. 47 (5):420.
100. Hewitt MJ, McPhail MJ, Possamai L, et al (2012) EUS-guided FNA for diagnosis of solid pancreatic neoplasms: a meta-analysis. Gastrointest Endosc. 75 (2):319-331.
101. LeBlanc JK, Ciaccia D, Al-Assi MT, et al (2004) Optimal number of EUS-guided fine needle passes needed to obtain a correct diagnosis. Gastrointest Endosc. 59 (4):475-481.
102. De Robertis R, Martini PT, Demozzi E, et al (2015) Diffusion-weighted imaging of pancreatic cancer. World J Radiol. 7 (10):319.
103. Niu X, Das SK, Bhetuwal A, et al (2014) Value of diffusion-weighted imaging in distinguishing pancreatic carcinoma from mass-forming chronic pancreatitis: a meta-analysis. Chin Med J (Engl). 127(19):3477-82.
104. Siddiqui N, Vendrami CL, Chatterjee A, Miller FH (2018) Advanced MR Imaging Techniques for Pancreas Imaging. Magn Reson Imaging Clin N Am. 26 (3):323-344.
105. Hsu W-L, Chang S-M, Wu P-Y, Chang CC (2018) Localized autoimmune pancreatitis mimicking pancreatic cancer: Case report and literature review. J Int Med Res. 46 (4):1657-1665.
106. Cao Z, Tian R, Zhang T, Zhao Y (2015) Localized autoimmune pancreatitis: report of a case clinically mimicking pancreatic cancer and a literature review. Medicine (Baltimore). 94(42):1656.
107. Díte P, Uvírová M, Bojková M, et al (2014) Differentiating autoimmune pancreatitis from pancreatic cancer. Minerva Gastroenterol Dietol. 60 (4):247-253.
108. Adsay NV (2008) Cystic neoplasia of the pancreas: pathology and biology. J Gastrointest Surg. 12 (3):401-404.
109. Procacci C, Megibow AJ, Carbognin G, et al (1999) Intraductal papillary mucinous tumor of the pancreas: a pictorial essay. Radiographics. 19 (6):1447-1463.
110. Machado NO, Al Qadhi H, Al Wahibi K (2015) Intraductal papillary mucinous neoplasm of pancreas. N Am J Med Sci. 7 (5):160.
111. Stark A, Donahue TR, Reber HA, Hines OJ (2016) Pancreatic cyst disease: a review. JAMA. 315 (17):1882-1893.
112. Megibow AJ, Baker ME, Morgan DE, et al (2017) Management of incidental pancreatic cysts: a white paper of the ACR Incidental Findings Committee. J Am Coll Radiol. 14 (7):911-923.
113. Kim KW, Park SH, Pyo J, et al (2014) Imaging features to distinguish malignant and benign branch-duct type intraductal papillary mucinous neoplasms of the pancreas: a meta-analysis. Ann Surg. 259 (1):72-81.
114. Tanaka M, Chari S, Adsay V, et al (2006) International consensus guidelines for management of intraductal papillary mucinous neoplasms and mucinous cystic neoplasms of the pancreas. Pancreatology. 6 (1-2):17-32.
115. Kucera JN, Kucera S, Perrin SD, et al (2012) Cystic lesions of the pancreas: radiologic-endosonographic correlation. Radiographics. 32 (7):283-301.
116. Tanaka M, Fernandez-Del Castillo C, Kamisawa T, et al (2017) Revisions of international consensus Fukuoka guidelines for the management of IPMN of the pancreas. Pancreatology. 17(5):738-753.
117. Kawamoto S, Horton KM, Lawler LP, Hruban RH, Fishman EK (2005) Intraductal papillary mucinous neoplasm of the pancreas: can benign lesions be differentiated from malignant lesions with multidetector CT? Radiographics. 25 (6):1451-1468.
118. Castelli F, Bosetti D, Negrelli R, et al (2013) Multifocal branch-duct intraductal papillary mucinous neoplasms (IPMNs) of the pancreas: magnetic resonance (MR) imaging pattern and evolution over time. Radiol Med. 118 (6):917-929.
119. Kang KM, Lee JM, Shin CI, et al (2013) Added value of diffusion-weighted imaging to MR cholangiopancreatography with unenhanced MR imaging for predicting malignancy or invasiveness of intraductal papillary mucinous neoplasm of the pancreas. J Magn Reson Imaging. 38 (3):555-563.
120. Gourgiotis S, Ridolfini M, Germanos S (2007) Intraductal papillary mucinous neoplasms of the pancreas. Eur J Surg Oncol. 33 (6):678-684.
121. Palmucci S, Trombatore C, Foti PV, et al (2014) The utilization of imaging features in the management of intraductal papillary mucinous neoplasms. Gastroenterol Res Pract. 2014:765451.
122. Hruban RH, Takaori K, Klimstra DS, et al (2004) An illustrated consensus on the classification of pancreatic intraepithelial neoplasia and intraductal papillary mucinous neoplasms. Am J Surg Pathol. 28 (8):977-987.
123. Lee KH, Lee S-J, Lee JK, et al (2014) Prediction of Malignancy With Endoscopic Ultrasonography in Patients With Branch Duct–Type Intraductal Papillary Mucinous Neoplasm. Pancreas. 43 (8):1306-1311.
124. Takanami K, Hiraide T, Tsuda M, et al (2011) Additional value of FDG PET/CT to contrast-enhanced CT in the differentiation between benign and malignant intraductal papillary mucinous neoplasms of the pancreas with mural nodules. Ann Nucl Med. 25 (7):501-510.
125. Bruno MA, Walker EA, Abujudeh HH (2015) Understanding and confronting our mistakes: the epidemiology of error in radiology and strategies for error reduction. Radiographics. 35 (6):1668-1676.
126. Berbaum KS (2012) Satisfaction of search experiments in advanced imaging. In: Human Vision and Electronic Imaging XVII. International Society for Optics and Photonics. 82910.
127. Kumar B, Kanna B, Kumar S (2011) The pitfalls of premature closure: clinical decision-making in a case of aortic dissection. BMJ Case Rep. 0820114594.
128. Biggs AT (2017) Getting satisfied with "satisfaction of search": how to measure errors during multiple-target visual search. Atten Percept Psychophys. 79 (5):1352-1365.
129. Winter JM, Cameron JL, Lillemoe KD, et al (2006) Periampullary and pancreatic incidentaloma: a single institution's experience with an increasingly common diagnosis. Ann Surg. 243 (5):673.
130. Bruzoni M, Johnston E, Sasson AR (2008) Pancreatic incidentalomas: clinical and pathologic spectrum. Am J Surg. 195 (3):329-332.
131. Laffan TA, Horton KM, Klein AP, et al (2008) Prevalence of unsuspected pancreatic cysts on MDCT. AJR Am J Roentgenol. 191 (3):802-807.
132. de Jong K, Nio CY, Hermans JJ, et al (2010) High prevalence of pancreatic cysts detected by screening magnetic resonance imaging examinations. Clin Gastroenterol Hepatol. 8 (9):806-811.
133. Cloyd JM, Poultsides GA (2015) Non-functional neuroendocrine tumors of the pancreas: Advances in diagnosis and management. World J Gastroenterol. 21 (32):9512.
134. Gorelik M, Ahmad M, Grossman D, Grossman M, Cooperman AM (2018) Nonfunctioning Incidental Pancreatic Neuroendocrine Tumors: Who, When, and How to Treat? Surg Clin North Am. 98 (1):157-167.
135. Kawamoto S, Siegelman SS, Bluemke DA, Hruban RH, Fishman EK (2009) Focal fatty infiltration in the head of the pancreas: evaluation with multidetector computed tomography with multiplanar reformation imaging. J Comput Assist Tomogr. 33 (1):90-95.

136. Hague J, Amin Z (2006) Focal pancreatic lesion: can a neoplasm be confidently excluded? Br J Radiol. 79 (943):627-629.
137. Kim HJ, Byun JH, Park SH, et al (2007) Focal fatty replacement of the pancreas: usefulness of chemical shift MRI. AJR Am J Roentgenol. 188 (2):429-432.
138. Isserow JA, Siegelman ES, Mammone J (1999) Focal fatty infiltration of the pancreas: MR characterization with chemical shift imaging. AJR Am J Roentgenol. 173 (5):1263-1265.
139. Movitz D (1967) Accessory spleens and experimental splenosis. Principles of growth. Chic Med Sch Q. 26 (4):183-187.
140. Halpert B, Györkey F (1959) Lesions observed in accessory spleens of 311 patients. Am J Clin Pathol. 32 (2):165-168.
141. Mortelé KJ, Mortele B, Silverman SG (2004) CT features of the accessory spleen. AJR Am J Roentgenol. 183 (6):1653-1657.
142. Coquia SF, Kawamoto S, Zaheer A, et al (2014) Intrapancreatic accessory spleen: possibilities of computed tomography in differentiation from nonfunctioning pancreatic neuroendocrine tumor. J Comput Assist Tomogr. 38 (6):874.
143. Kim SH, Lee JM, Han JK, et al (2008) Intrapancreatic accessory spleen: findings on MR Imaging, CT, US and scintigraphy, and the pathologic analysis. Korean J Radiol. 9 (2):162-174.
144. Kim SH, Lee JM, Han JK, et al (2006) MDCT and superparamagnetic iron oxide (SPIO)-enhanced MR findings of intrapancreatic accessory spleen in seven patients. Eur Radiol. 16 (9):1887.
145. Herédia V, Altun E, Bilaj F, et al (2008) Gadolinium-and superparamagnetic-iron-oxide-enhanced MR findings of intrapancreatic accessory spleen in five patients. Magn Reson Imaging. 26 (9):1273-1278.
146. Ota T, Tei M, Yoshioka A, et al (1997) Intrapancreatic accessory spleen diagnosed by technetium-99m heat-damaged red blood cell SPECT. J Nucl Med. 38 (3):494-495.
147. Rijkers AP, Bakker OJ, Ali UA, et al (2017) Risk of pancreatic cancer after a primary episode of acute pancreatitis. Pancreas. 46 (8):1018-1022.